2010

# Role of pyridoxine 5'-phosphate oxidase in metabolism and transfer of pyridoxal 5'-phosphate

Sayali Karve
*Virginia Commonwealth University*

# ROLE OF PYRIDOXINE 5'-PHOSPHATE OXIDASE IN METABOLISM AND TRANSFER OF PYRIDOXAL 5'-PHOSPHATE

A dissertation submitted in partial fulfillment of the requirements for the degree of Master of Science at Virginia Commonwealth University.

by

SAYALI SUNIL KARVE

Bachelor of Pharmacy, Pune University, India, 2007

Director: MARTIN K. SAFO, PHD

ASSOCIATE PROFESSOR OF MEDICINAL CHEMISTRY

Virginia Commonwealth University

Richmond, Virginia

August, 2008

**ACKNOWLEDGEMENT**

This research project would not have been possible without the support of many people. I would start by thanking my advisor, Dr. Martin Safo, for his supervision, advice and guidance at every stage of the research as well as for giving me extraordinary research experience throughout the past one and a half years that I worked in the lab. He was always accessible and willing to help with the research in every way possible, which made the research smooth and rewarding.

I gratefully acknowledge Dr. Mohini Ghatge for helping me with protein expression, purification and kinetic studies. Her involvement with her originality has triggered and nourished my intellectual maturity that I will benefit from, for a long time to come. I am much indebted to her for her valuable advice in science discussions and furthermore for her constructive comments on this thesis. I am also thankful to Dr. Faik Musayev for teaching me the techniques of X-ray crystallography.

Many thanks go to Dr. Darrel Peterson and Dr. John Hackett, that in the midst of all their activities, they agreed to be the members of my defense committee. I was benefited by the advice and guidance from Dr. Peterson, who always kindly granted me his time even for answering some of my unintelligent questions about molecular biology.

It was nice to work with our research group members, Jigar, Soumya, Amit and Ashwini. I would especially like to mention Soumya and Jigar who inspired me in research and made working in the lab fun. I will always remember those long hours in the lab on weekdays and even on weekends. It was a great experience working in the Institute for Structural Biology and Drug Discovery, and I would like to thank all my friends here in the Institute, the Department of Medicinal Chemistry and VCU for always being helpful and resourceful.

I would especially like to mention my friends outside the Department, Kushal, Abhijeet, Varun, Jigar, Soumya, Soundarya, Hardik, Ronak, Ashutosh, Lopa, Margi and Vipul for always being there and believing in me. My parents and family deserve a special mention for their inseparable support and prayers. Where would I be without my family?

And last but not the least I would like to thank Department of Medicinal Chemistry and School of Pharmacy at VCU for giving me this opportunity to study here.

Table of Contents

Page

List of Tables

Page

List of Figures

Page

List of Abbreviations

| | |
|---|---|
| PN | Pyridoxine |
| PL | Pyridoxal |
| PM | Pyridoxamine |
| PNP | Pyridoxine 5'-phosphate |
| PLP | Pyridoxal 5'-phosphate |
| PMP | Pyridoxamine 5'-phosphate |
| PLK | Pyridoxal kinase |
| PNPO | Pyridox(am)ine 5'-phosphate oxidase |
| FMN | Flavin mononucleotide |
| SHMT | Serine hydroxymethyl transferase |
| NEE | Neonatal epileptic encephalopathy |
| Ni-NTA | $Ni^{+2}$-nitrilotriacetic acid |
| OD | Optical density |
| IPTG | Isopropyl β-D-thiogalactopyranoside |
| LB | Luria Bertani |
| PMSF | Phenyl methyl sulfonyl fluoride |
| SDS PAGE | Sodium dodecyl sulfate, polyacrylamide gel electrophoresis |
| DTT | Dithiothreitol |
| CD | Circular dichroism |
| $T_m$ | Melting temperature |
| EDTA | Ethylene diamine tetra acetic acid |

| | |
|---|---|
| BES | N, N-Bis (2-hydroxyethyl)-2-aminoethanesulfonic acid |
| HEPES | 4-(2-hydroxyethyl)-1-piperazine ethanesulfonic acid |
| TMAE | Trimethylaminoethyl |
| FP | Fluorescence polarization |
| AAT | Aspartate aminotransferase |
| FMi | Fluorescein 5- maleimide |
| LDH | Lactate dehydrogenase |
| THF | Tetrahydrofolate |
| YT | Yeast Tryptone |

# ABSTRACT

Deficiency of vitamin $B_6$ due to mutations in key $B_6$ metabolizing enzymes is suspected to contribute to several pathologies. Vitamin $B_6$ in its active form, pyridoxal 5'-phosphate (PLP) is a cofactor for over 140 known $B_6$ requiring (or PLP-dependent) enzymes, that serve vital roles in many biochemical reactions. There are three primary vitamin $B_6$ forms, pyridoxine (PN), pyridoxamine (PM) and pyridoxal (PL) which are phosphorylated to pyridoxine 5'-phosphate (PNP), pyridoxamine 5'-phosphate (PMP) and PLP respectively. Pyridoxal kinase (PLK) and pyridoxine 5'-phosphate oxidase (PNPO) are the key enzymes involved in both salvage and *de novo* pathways of PLP biosynthesis. Mutations in these enzymes are one of the most important causes of PLP deficiency, apart from dietary insufficiency of vitamin $B_6$ and drug inhibition of PLK and PNPO. One of our objectives is to understand the molecular basis of reduced catalytic activity of PNPO in case of the R95C homozygous missense natural mutant, which leads to the PLP deficiency and the debilitating disease, neonatal epilepsy encephalopathy. Using site-directed mutagenesis, circular dichroism, enzyme kinetics and fluorescence spectroscopy, we have shown that the reduced enzymatic activity exhibited by PNPO R95C mutant is due to reduced binding affinity of the oxidase cofactor, flavin mononucleotide (FMN), which is required by the enzyme for oxidizing the inactive $B_6$ vitamers into the active PLP.

High concentrations of $B_6$ are linked to neurotoxic effects, which can be attributed to the highly reactive aldehyde group of PLP which reacts with many nucleophiles in the cell. This reactivity is most likely why the *in vivo* concentration of "free" PLP is about 1 μM, raising the intriguing question of how the cell supplies sufficient PLP to meet the requirements of the

numerous $B_6$ dependent enzymes. Our second objective is to determine how despite the low *in vivo* concentration of free PLP, enough of this co-factor is made available to activate PLP-dependent enzymes. We have used affinity pull down assays, fluorescence polarization and enzyme kinetics to show that PNPO forms specific interactions with $B_6$ enzymes with dissociation constants less than 1 μM. We also show that transfer of PLP from PNPO possibly occurs by compartimentalization or channeling. Although, channeling is a controversial subject, it offers an efficient, exclusive, and protected means of delivery of the highly reactive PLP.

# Chapter 1

# General Introduction

**1.1 $B_6$ vitamers:** Vitamin $B_6$, a water soluble vitamin belonging to the B complex family, is critical to maintain biochemical homeostasis. There are six natural forms of vitamin $B_6$: pyridoxine (PN), pyridoxal (PL), pyridoxamine (PM), and their phosphorylated analogs viz. pyridoxine 5'-phosphate (PNP), pyridoxal 5'-phosphate (PLP) and pyridoxamine 5'-phosphate (PMP), respectively. [1,2] (Figure 1) Of these, PLP and to a lesser extent PMP are the metabolically active forms that are used as cofactors by vitamin $B_6$ dependent enzymes.[3,4]

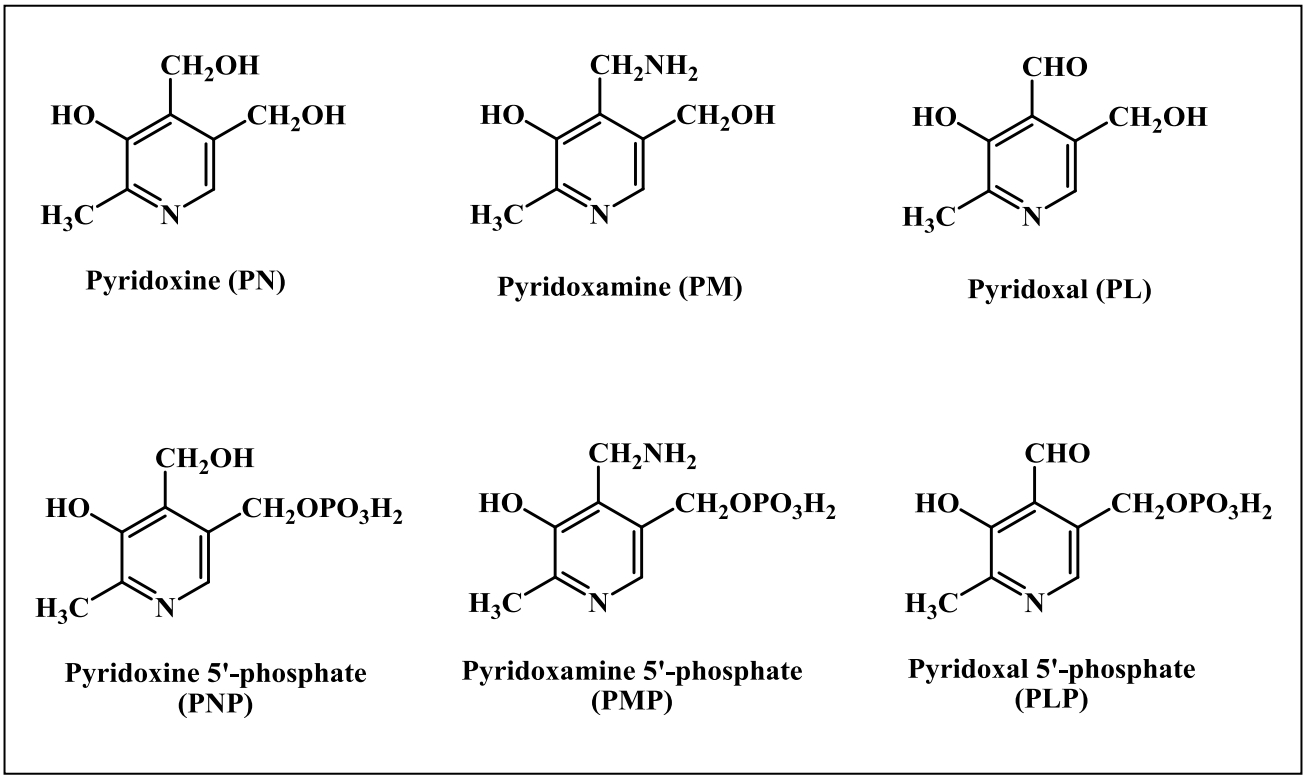


**Figure 1:** Structures of $B_6$ vitamers

**1.2 Biosynthetic pathways for vitamin $B_6$:** Prokaryotes such as bacteria synthesize PNP, PMP and PLP by a *de novo* pathway from erythrose 4-phosphate (E4P).[5] Eukaryotes cannot synthesize PLP by the *de novo* pathway and depend on the primary dietary $B_6$ vitamers PN, PL and PM for the synthesis of PLP via the so called salvage pathway. Two enzymes contribute to the salvage pathway: an ATP dependent pyridoxal kinase (PLK) and a flavin mononucleotide (FMN) dependent pyridoxine 5'-phosphate oxidase (PNPO). PLK phosphorylates 5' alcohol group of PN, PL and PM to form PNP, PLP and PMP respectively. (Figure 2) PNP and PMP are further oxidized to PLP by PNPO.[6] (Figure 2) PLP is then transferred to apo $B_6$ dependent enzymes, which catalyze various biochemical reactions. PLP, PNP and PMP are dephosphorylated by phosphatase class of enzymes to PL, PN and PM respectively. (Figure 2)

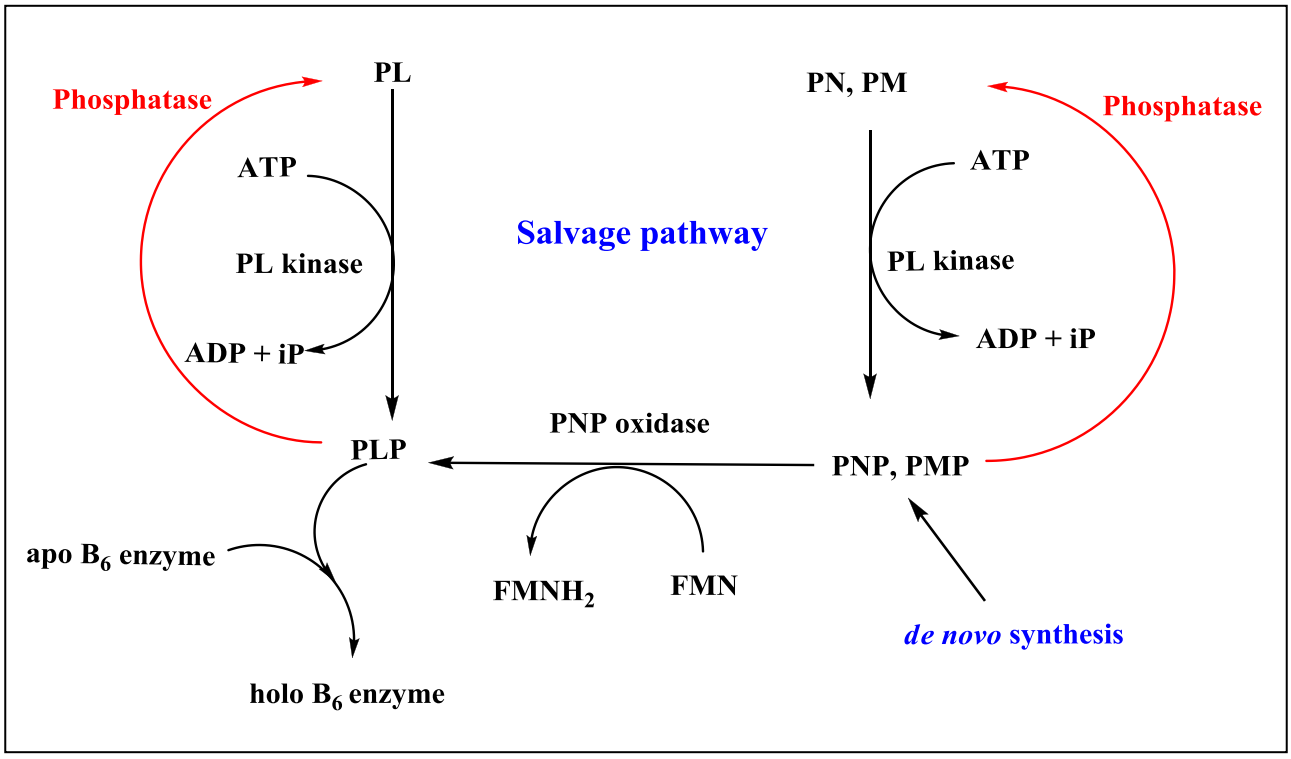


**Figure 2:** Biosynthesis of PLP

**1.3 Pyridoxal Kinase (PLK):** This ATP dependent enzyme phosphorylates 5'-alcohol of PM, PL and PN with γ-phosphate of ATP to form PMP, PLP and PNP respectively.[1, 8] (Figure 3) The enzyme is a homodimer with one active site per subunit. Pyridoxal kinases have been isolated from mammalian and bacterial sources,[9, 10] sharing 24-90% sequence homology between them.[11, 12] Eukaryotic enzymes have been found to have broad substrate specificity tolerating modifications at the 4'-position of the vitamin $B_6$ forms.[13, 14] Pyridoxal kinase requires $Mg^+$ or $K^+$ for activity.[10]

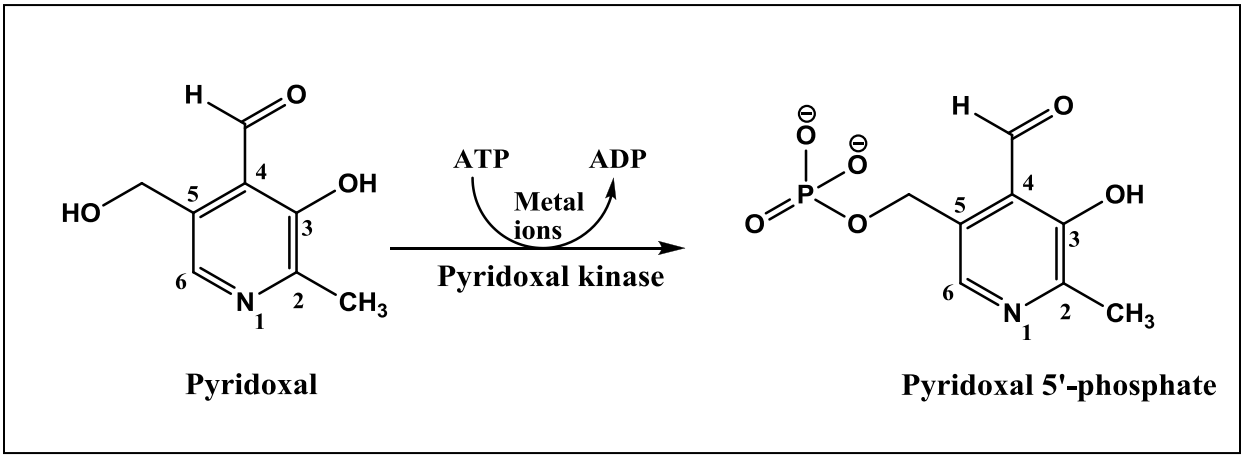


**Figure 3:** Phosphorylation of 5' alcohol of PL to PLP by pyridoxal kinase

**1.4 Pyridoxine 5'-phosphate oxidase (PNPO):** This flavin mononucleotide (FMN) dependent enzyme catalyzes the terminal step in the *de novo* vitamin $B_6$ biosynthesis in *E. coli* and is a part of the salvage pathway in *E. coli* and mammalian cells.[6, 15, 16] The catalysis involves oxidation of 4' hydroxyl group of PNP or 4'-amino group of PMP to form PLP. Two electrons are transferred to FMN, as a hydride in this process, forming $FMNH_2$. These electrons are eventually transferred to molecular oxygen to form hydrogen peroxide and FMN is regenerated.[15, 16, 17] (Figure 4) The enzyme is sluggish with a low catalytic rate constant ranging from 0.2 $sec^{-1}$ to 0.8 $sec^{-1}$ and $K_m$ values in the low micromolecular range for both the substrates PNP and PMP.[16, 17, 18]

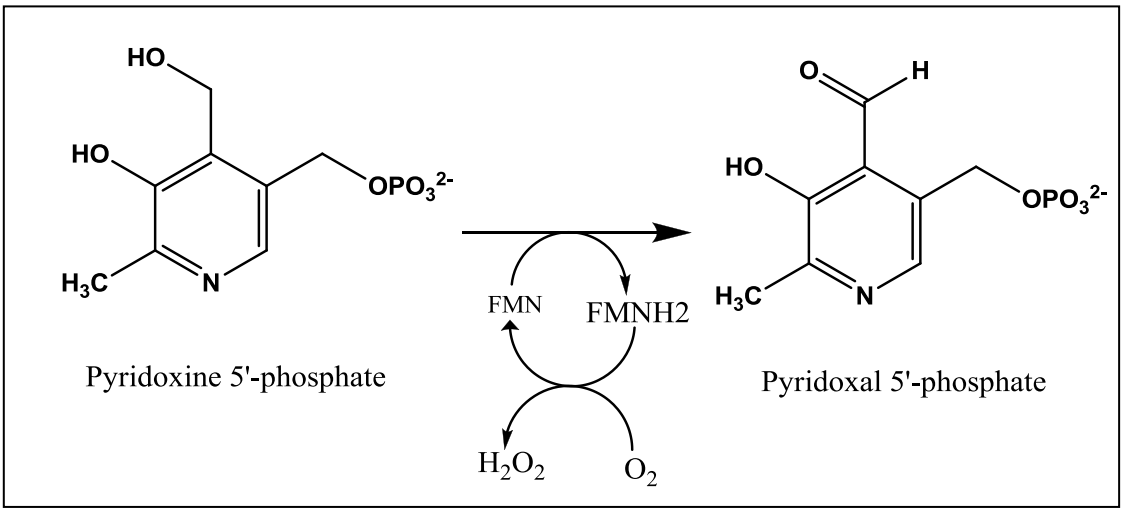


**Figure 4:** Oxidation of PNP to PLP by pyridoxine 5'-phosphate oxidase

PNPO is a homodimer with one active site per monomer. Each monomer (M.W. 29,985 Da for Human enzyme) folds into an eight stranded β-sheet surrounded by five α-helical structures. There are two FMN binding sites at the dimer interface where the cofactor interacts non-covalently with both the subunits.[15, 16, 17] (Figure 5) PNP or PMP bind at the *re*-face of N5 of the bound FMN. The isoalloxazine ring of FMN is coplanar with the pyridine ring of PNP and the two are separated by ~ 3.4 Å.[19] (Figure 6) The product PLP has a greater affinity for the active site than either of the substrates PNP or PMP, suggesting that it function as an inhibitor of the enzyme.[18, 20- 23] The human, *E. coli* and yeast enzymes share 54% sequence similarity, with 28% sequence identity, but the overall structure as well as the active sites are nearly identical.[15, 16, 24] (Figure 7)

**Non-catalytic site for PLP:** *In vitro* studies have shown that PNPO binds a second molecule of PLP tightly at a non-catalytic site. Enzymatic activities of PLP tightly complexed with PNPO were measured and compared with the activity of PNPO alone. PLP bound at this site does not inhibit the catalytic activity of the enzyme. Thus, this binding is assumed to be different than product inhibition by PLP which occurs at the active site. Also apo-enzyme has been observed to bind PLP with equal affinity as that of holo, and removal of the cofactor FMN did not influence binding. Even though this PLP remains bound to the enzyme during size exclusion chromatography it is readily transferred to apo serine hydroxymethyl transferase (SHMT)[16, 25]. Structural studies showed a secondary bound PLP at the surface of the protein, and about 11 Å from the active site. [19] It's not certain whether this secondary bound PLP site is the functionally observed non-catalytic site.

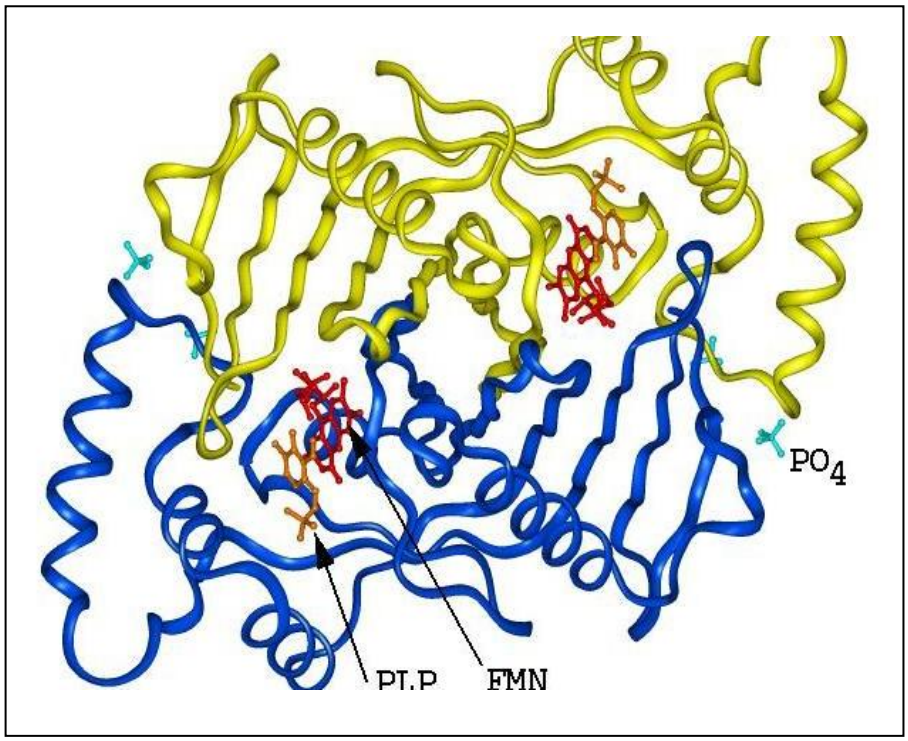


**Figure 5:** Homodimeric structure of *E. coli* PNPO with FMN and PLP bound at the active site

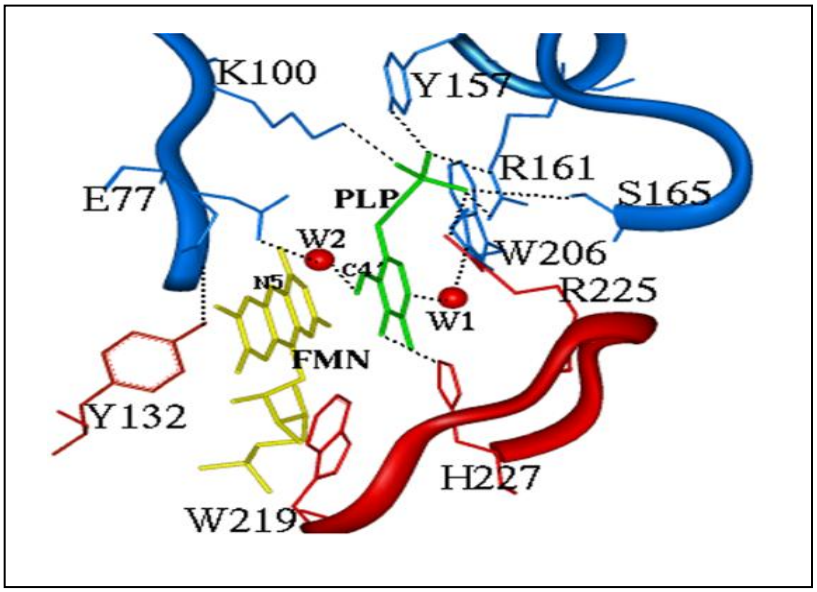


**Figure 6:** Active site structure of *E. coli* PNPO

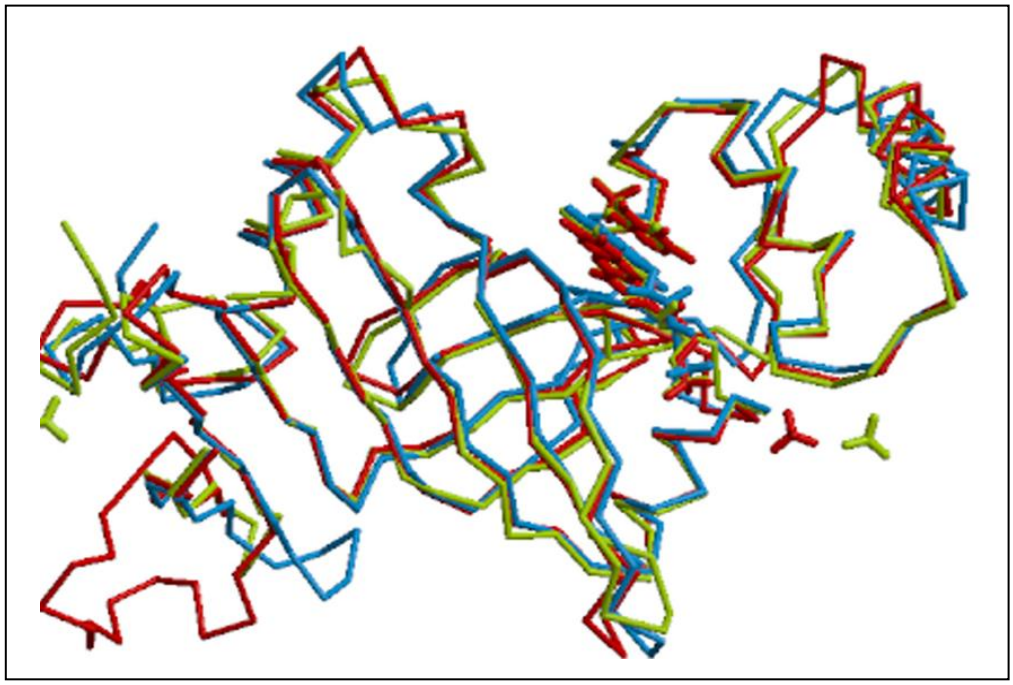

**Figure 7: Least square superimposition of PNPO from various sources:** Human PNPO (red); *E. coli* (yellow) and yeast PNPO (cyan)

**1.5 Vitamin $B_6$ Dependent Enzymes:** PLP serves diverse functions as a cofactor for over 140 vitamin $B_6$ dependent enzymes that include oxidoreductases, transferases, isomerases, lyases and hydrolases, with functions of many others unknown.[26] In addition to the catalytic mechanisms, reaction specificity and folding mechanisms, the 3D structures of several of these PLP-dependent enzymes are known.[27] The enzymes catalyze several important biochemical reactions such as amino acid and lipid metabolism, carbohydrate breakdown, neurotransmitter synthesis, heme synthesis and nucleic acid synthesis.[26-30] The enzymatic activities of these vitamin $B_6$ dependent enzymes contribute to about 4% of all classified activities. Of particular interest in these is their role in brain metabolism since the synthesis of most neurotransmitters, including GABA (pathway A), dopamine, epinephrine, norepinephrine, serotonin (pathways B and C), serine (pathway D) and histamine (pathway E) involves the $B_6$ dependent enzymes. (Figure 8) Concentration of PLP in brain depends on salvage pathway of synthesis since it does not cross the blood brain barrier easily. Since the PLP dependent enzymes compete for PLP in the brain, disruption of the salvage pathway could result in improper functioning of these enzymes. Deficiency of neurotransmitters due to improper functioning of PLP-dependent enzymes has been documented in several neurological disorders including epilepsy, Parkinson's disease, Alzheimer's disease and schizophrenia.[31-39]

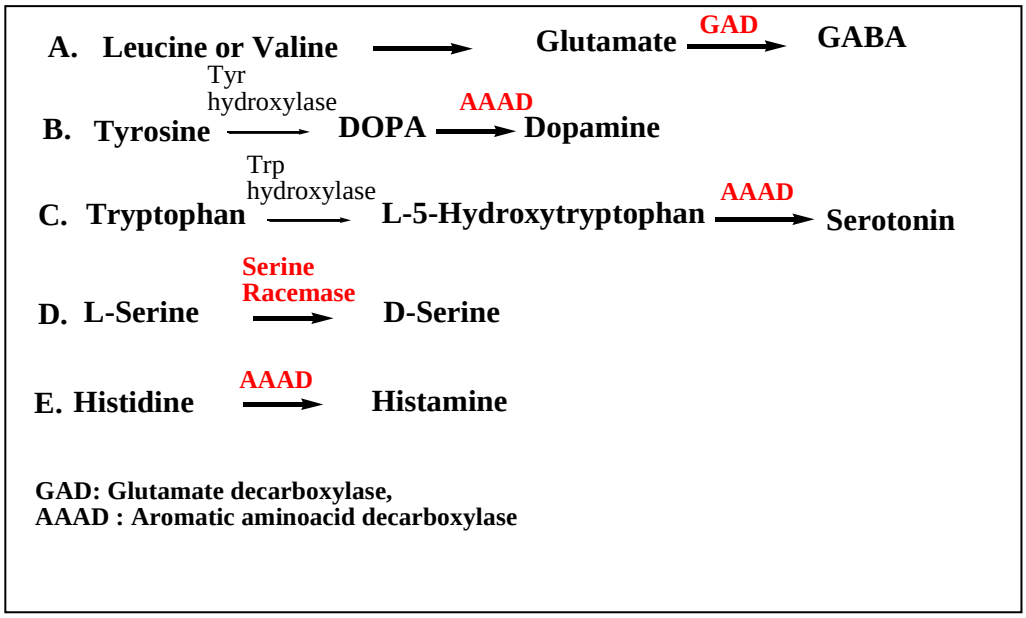


**Figure 8:** Synthesis of neurotransmitters by vitamin $B_6$ dependent enzymes

The aldehyde functionality of PLP allows it to form Schiff linkages with the ε-amino group of lysine residues at the active sites of the PLP dependent enzymes, the linkages termed internal aldimines. The phosphate of PLP interacts with a glycine rich loop present in the active site. Upon binding of the amino acid substrate, the lysine is exchanged for amino group of the substrate which forms Schiff base with PLP. This is called external aldimine, where α-amino group of the amino acid substrate acts is a nucleophile that attacks the carbon of the Schiff base of the internal aldimine and displaces the lysine residue.[40, 41] (Figure 9) The conversion from internal to external aldimine takes place via formation of a germinal diamine where PLP interacts with amino groups of both the substrate and the internal lysine residue.

The PLP dependent enzymes are classified into at least 5 different classes based on amino acid sequence comparison, predicted secondary structure elements and available 3D structural information as Fold type I (e.g. aspartate aminotransferase, serine hydroxymethyl transferase,

threonine aldolase), Fold type II (e.g. tryptophan synthase), Fold type III (e.g. ornithine decarboxylase), Fold type IV (e.g. alanine aminotransferase) and finally fold type V (e.g. glycogen phosphorylase).[42-44]

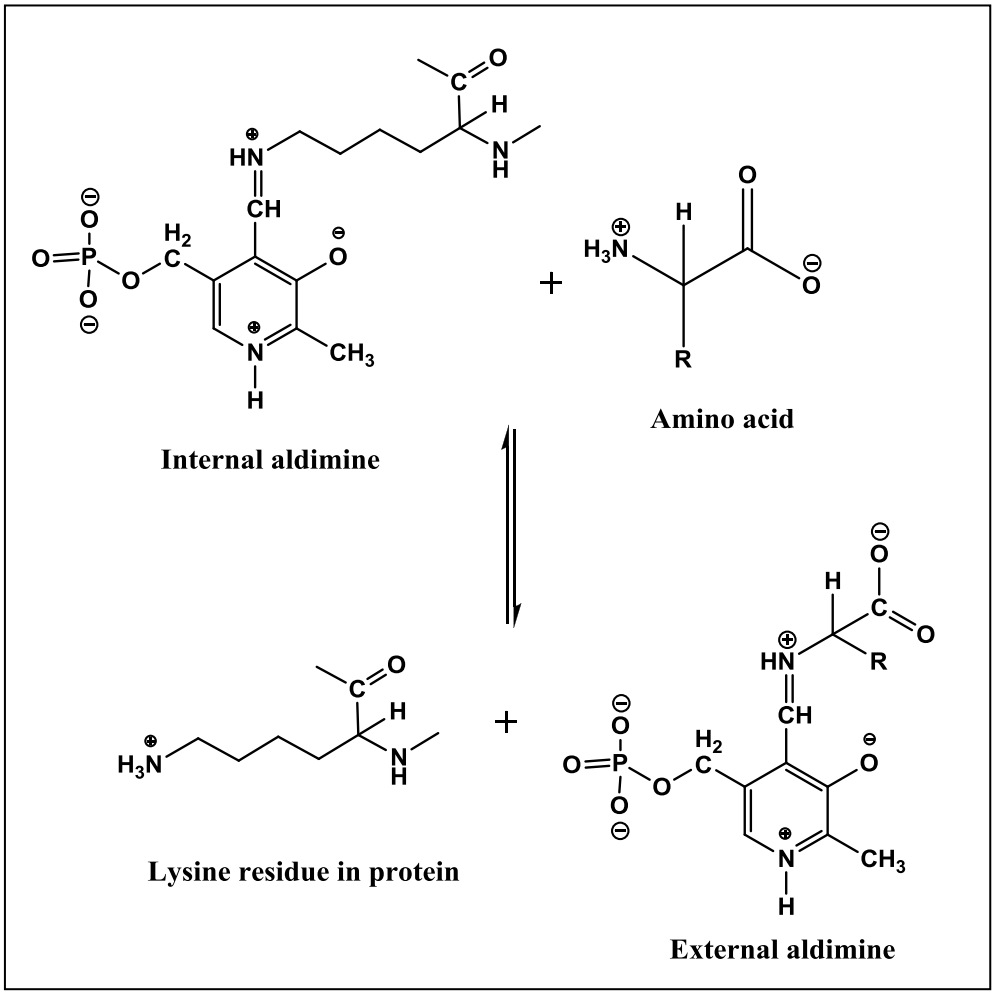


**Figure 9:** Internal and external aldimines formed by PLP

**1.6 Deficiency of PLP:** Deficiency of isolated vitamin $B_6$ is uncommon; it usually occurs in combination with deficiencies of other B-complex vitamin types. However, because of its wide variety of functions in the body as a cofactor, vitamin $B_6$ deficiency results in a broad spectrum of impaired activities including several neurological and non neurological disorders. The important causes of PLP decifiency are considered as (i) dietary insufficiency, (ii) drugs or compounds that inhibit PLK or PNPO, the two enzymes involved in PLP metabolism, or (iii) impairment of PLK or PNPO due to pathogenic mutations.[45, 46]

**1.6.A Dietary insuffiency:** The dietary insufficiency may produce symptoms such as seizures, sleeplessness, headache, restlessness, agitation, tremors, and hallucination. However, since vitamin $B_6$ is present in almost all food types including potatoes, bananas, beans, seeds, nuts, red meat, poultry, fish, eggs, spinach, and fortified cereals, the deficiency of PLP due to dietary insufficiency is rare.

**1.6.B Inhibition by drugs:** Some medicines as well as natural substances, on the other hand, have the ability to antagonize the actions of vitamin $B_6$. Some classes of substances achieve the PLP antagonistic effects by inhibing activities of PLK and PNPO.[47, 48] Acute inhibition of these enzymes can cause convulsions, unconsciousness, paralysis of leg and even death apart from the less severe symptoms such as seizures, headache and agitation.[49] Some examples of drugs found to be responsible for this are ginkgotoxin (4'-O-methylpyridoxine), theophylline, caffeine, theobromine, mesalamine, epinephrine and lamotrigine. For example, a plasma concentration of theophylline greater than 110 μM is reported to be associated with these symptoms.[50] Another class of substances that are shown to cause deficiency of PLP include progesterone and estrogen containing oral contraceptives. These have been observed to increase the demand for vitamin $B_6$ by increasing the substrate load of PLP dependent enzymes or cause

redistribution of PLP among its apoenzymes.[51] Alcohol acts as a vitamin $B_6$ inhibitor by decreasing the absorption of PLP.[52] The deficiency of vitamin $B_6$ caused by factors such as dietary insufficiency and drug inhibition can be treated by vitamin $B_6$ supplements, co-administering drugs with vitamin $B_6$ or by stopping treatment with the vitamin $B_6$ deficiency causing drugs.

**1.6.C Mutations in PLK and PNPO:** A more severe deficiency of vitamin $B_6$ can occur as a result of mutations in genes producing the enzymes involved in vitamin $B_6$ metabolism. Human PLK and PNPO genes are situated on chromosomes 21q22.3 and 17q21.2 respectively.[53] In a study by Mills *et al*, PNPO was sequenced in patients showing deficiency of the enzyme. Homozygous missense, splice site and stop codon mutations were identified, all of which showed reduced or abolished catalytic efficiency of the enzyme, leading to PLP deficiency.[54] Several other studies have linked the possibility of other neurological disorders such as Alzheimer's disease, schizophrenia, Parkinson's disease, attention deficit hypersensitivity disorder, to the PLP deficiency due to its effect on neurotransmitter synthesis.[55, 56] Some of the natural mutations observed in PLK and PNPO with their natural phenotypes are listed in Table 1. The use of vitamin $B_6$ supplementation to treat PLP deficiency caused by pathogenic mutations in PNPO or PLK has shown conflicting results. Administration of PN alone to patients with NEE showed no relief, whereas administration of PL/PLP showed better results. This further supports the defect in PNPO. The difference between PN and PLP in seizure control has also been noted in a patient whose seizures were controlled by PLP but not with PN. It is quite clear that therapy with PN or PM in patients with a defective PNPO will not be successful and administration of PLP as currently the most effective choice of treatment.[57]

.

**Table 1:** Mutations in PNPO and PLK along with their natural phenotypes

| **Pyridoxine 5'-Phosphate Oxidase** | | **Pyridoxal Kinase** | |
|---|---|---|---|
| **Mutation** | **Phenotype** | **Mutation** | **Phenotype** |
| R116Q | NA* | P129P | NA |
| R229W | Lethal | S216F | NA |
| X262Q | Lethal | S213S | None |
| E50K | More active | R224P | None |
| R95C | Lethal | | |
| R95H | Lethal | | |

**1.7 Toxicity of PLP:** PLP contains a very reactive aldehyde group at the 4' position that reacts with virtually all nucleophiles and proteins in the cell including non vitamin $B_6$ dependent proteins, leading to neuropathies. It forms aldimines with primary and secondary amines. Some of the complexes formed by PLP are shown in Figure 10. It is often used as a protein labelling agent because of its reactivity with the ε-amino group of lysyl residues in proteins. Vitamin $B_6$ does not produce any toxicities at low concentrations. The current recommended dietary allowance of PLP is 1.3 to 2 mg/day in the United States. Toxicities are observed usually when the concentration exceeds 200 mg/day.[58] The levels of $B_6$ could be raised as a result of an environmental insult or genetic defects. The toxicity with PLP is known to cause sensory as well as motor neuropathies leading to numbness in hands and feet leading to difficulty in walking. Although some cases with acute, profound and permanent neuropathies have been noted, the sensory neuropathies are usually reversible when supplementation is stopped.[59] Administration of high doses of PLP to rats and dogs has shown to produce hind leg paralysis, focal damage of peripheral nerves and selective degeneration of the spinal cord.[60]

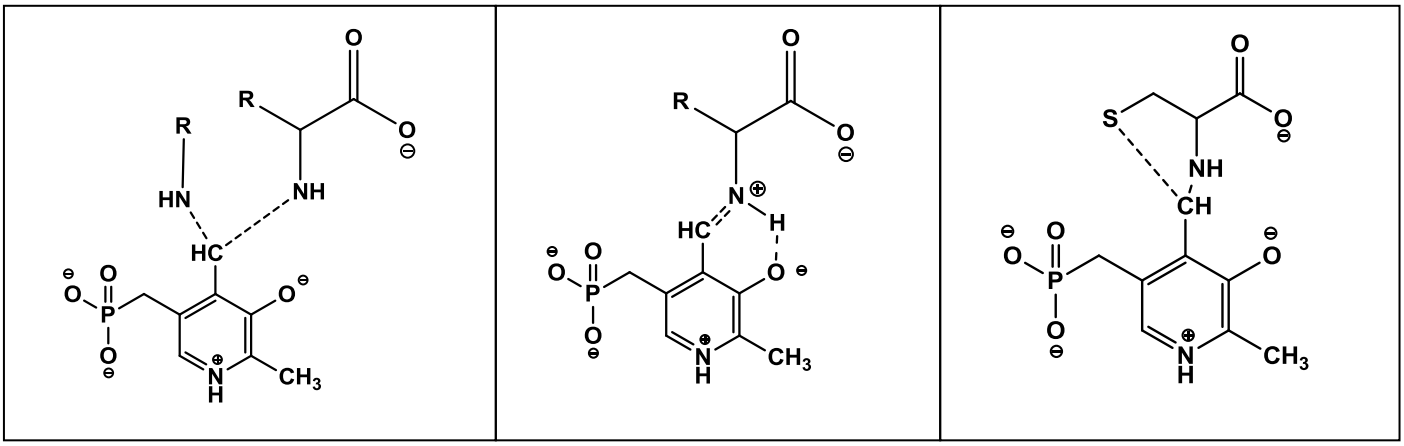


**Figure 10:** Nucleophillic adducts of PLP

**1.8 Homeostatic regulation of vitamin $B_6$ levels:** The pool of free PLP *in vivo* is maintained at a very low concentration in the body, presumably to prevent toxic buildup. Regulation of PLP synthesis by pyridoxal kinase and PNPO is a proposed mechanism. Zhao and Winkler observed inhibition of *E. coli* PNPO activities by product PLP with the $K_i$ of 8 µM.[18] In another study by our group, significant MgATP substrate inhibition of *E. coli* PLK was observed in presence of PNP or PLP.[12] Another well established mechanism for maintaining low levels of free PLP is dephosphorylation of PLP by phosphatases. These $Mg^{2+}$ dependent enzymes carry out dephosphorylation of PLP back into pyridoxal. The catalysis is carried out by both free as well as membrane bound phosphatases with $k_{cat}$ values at least 30-fold higher than the PLP producing enzymes. The PLP specific phosphatase has a $K_m$ of ~2.5 µM for PLP[62]. Catalytic conversion of pyridoxal to 4-pyridoxic acid, by aldehyde oxidase and NAD-dependent dehydrogenase is another mechanism of regulation of free PLP concentration[63, 64]. The concentration of free PLP is maintained as low as 1 µM in eukaryotic cells. Nevertheless despite this low level of free PLP, enough PLP is made available to vitamin $B_6$ dependent enzymes. This raises the intriguing question of how the cell supplies sufficient PLP for the numerous $B_6$ enzymes.

**1.9 PLP transfer:** The question of how PLP adds to apo enzymes has been strongly debated and difficult to unravel. The problem has been noted previously by many researchers during their work on the enzymes involved in PLP metabolism.[22, 65, 66] It seems that for successful activation of apo vitamin $B_6$ dependent enzymes without producing any toxic effects, the PLP produced by $B_6$ metabolizing enzymes should be transferred to the apo enzymes as quickly as possible.

It has been studied for many years how a product or an intermediate of one enzymatic reaction is transferred to another enzyme to carry out subsequent reactions. Enzymes have been observed to follow two basic pathways by which the transfer takes place, viz. non-channeled and channeled. Based on these, there could be two possible mechanisms of PLP transfer to the apo enzymes.

**Mechanism 1:** A non-channeled mechanism, where PL kinase and PNPO release PLP into the solution in cell and the pool of free PLP reacts with apoenzymes to activate them.

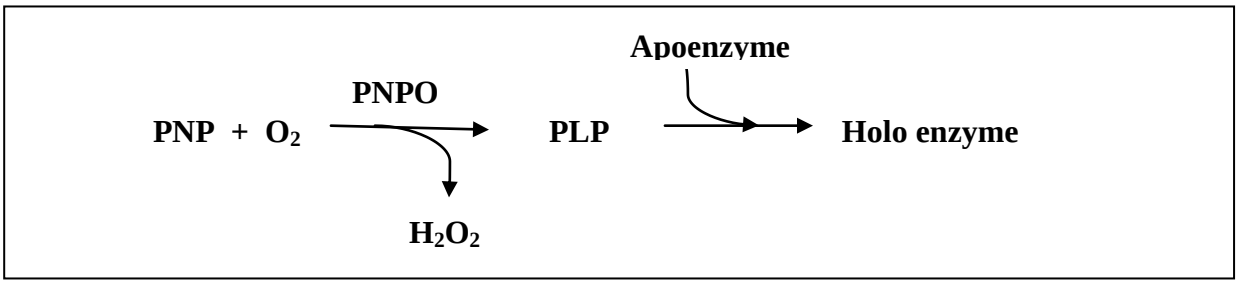


However, the reactive nature of PLP, the high $k_{cat}$ values of phosphatases and feedback inhibition of the metabolising enzymes by product PLP decrease the feasibility of this route of transfer.

**Mechanism 2:** Channeled mechanism, where PLP is transferred directly from either PLK and PNPO to apoenzymes and activate them.

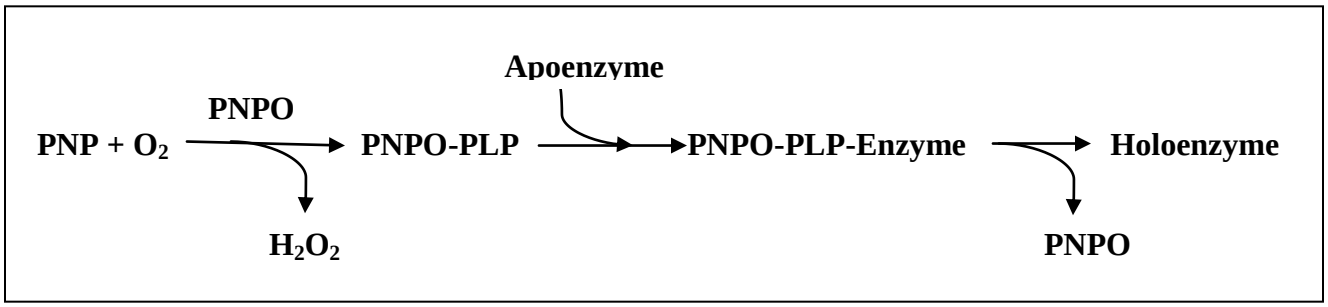


PLP transferred by this method has the advantages of shortening the reaction time and sequestrating the reactive PLP from bulk solution, protecting it from hydrolysis by phosphatases. This method of PLP transfer also prevents interaction of free PLP to enzymes and proteins other than $B_6$ dependent enzymes.

**1.10 Rationale and specific aims:** Pyridoxal 5'-phosphate, the metabolically active form of vitamin $B_6$, is an important cofactor for many enzymes that catalyze over 140 biochemical reactions, particularly reactions involved in the synthesis of neurotransmitters. Deficiency of PLP is therefore implicated in several neurological disorders such as neonatal epileptic encephalopathies, Parkinson's disease, Alzheimer's disease, attention deficit hypersensitivity disorders, Down's syndrome to name a few. Of these, deficiency of PLP function has been documented in several cases of neonatal epileptic encephalopathies. The deficiency of PLP in NEE has been found to be mainly due to mutations in PNPO, an enzyme responsible for the catalysis of the terminal step of PLP synthesis. However, mutations in PLK could also be involved in neurological disorders. Dietary insufficiency of vitamin $B_6$ or inhibition of PLK or PNPO activity by drugs are also known to result in PLP deficinecy with neurotoxic effects. Our first goal is to understand how a homozygous missense mutation in human PNPO, R95C affects its catalytic activity.

PLP has a reactive aldehyde function which interacts with almost all nucleophiles including proteins other than vitamin $B_6$ enzymes, which may cause neurological as well as non-neurological toxicities. The *in vivo* concentration of free PLP is thus maintained very low (~1-2 µM) by mechanisms such as feedback inhibition of PLK and PNPO by PLP, hydrolysis of free PLP back into PL by phosphatases and conversion of free PLP into 4-pyridoxic acid. It is, therefore, very interesting to determine how in spite of the low concentrations, PLP gets transferred from PNPO and PLK to the vitamin $B_6$ dependent enzymes. Our second goal is to study how PLP synthesized by PNPO is transferred to the vitamin $B_6$ dependent enzymes.

There are two specific aims:

1. Determine the molecular basis of reduced activity of human pyridoxine 5'-phosphate oxidase due to a homozygous missense R95C mutation.

2. Determine the mechanism of transfer of PLP from pyridoxine 5'-phophate oxidase to vitamin $B_6$ dependent enzymes.

# Chapter 2

# Molecular basis of reduced catalytic activity of human pyridoxine 5'-phosphate oxidase by the R95C mutation

**2.1 Introduction:** Neonatal epileptic encephalopathy (NEE) is a severe disorder which manifests a few hours after birth with intractable seizures usually unresponsive to conventional anticolvulsant treatment.[54] Observed mainly in Turkish and Asian populations, NEE shows symptoms such as fetal distress, hypoglycemia, anemia, acidosis and asphyxia.[54, 68] Analysis of cerebrospinal fluid and urine of patients shows decreased activity of vitamin $B_6$ enzymes. The surviving children are usually mentally retarded and show an abnormal dependence on vitamin $B_6$ in the form of pyridoxal 5'-phosphate (PLP).[69] Studies have also shown that treatment of seizures resulting in NEE responded to PLP while PNP (/PMP) or PN (/PM) had no effect.[54, 68] This led to the suggestion that the disorder might involve defective enzymes for PLP biosynthesis. Sequencing of PNPO coding genes in patients with NEE have identified several pathogenic mutations, including homozygous missense (R95C, R95H, R229W), stop codon (X262Q) or splice site (IVS3-1g > a) mutations.[57, 70-72] Of these, our lab has previously studied R229W and R229Q mutations, which show highly reduced catalytic activity as compared to the wild type.[69] The stop codon and splice site mutations on the other hand resulted in null PNPO activity.

PNPO, the homodimeric enzyme involved in catalysis of the terminal step of PLP biosynthesis, has been purified from *E. coli*, humans, rabbit, yeast and several other species with the catalytic site conserved.[16] FMN is the cofactor which is critical for the catalytic activity of

the enzyme and is non-covalently attached to each subunit at the dimer interface. FMN is coplanar with the substrate PNP and takes up two electrons in the form of a hydride from PNP to convert it to PLP[19, 20].

The present study is aimed at understanding on a molecular level why the PNPO R95C mutation leads to reduced oxidase activity with concomittant NEE. The catalytic site of human PNPO (hPNPO) is shown in Figure 11. In the wild-type structure, the Arg-95 residue forms salt bridge/hydrogen bond interactions with the phosphate side chain of the FMN molecule present in the catalytic site. Figure 11 also shows a putative position of Cys95 replacement of Arg95. We hypothesize that the salt bridge/hydrogen bond interactions would be lost when the Arg group is replaced with Cys group. This loss of interactions may result in decreased affinity of the enzyme towards its cofactor, FMN, which may be the cause of its reduced catalytic efficiency.

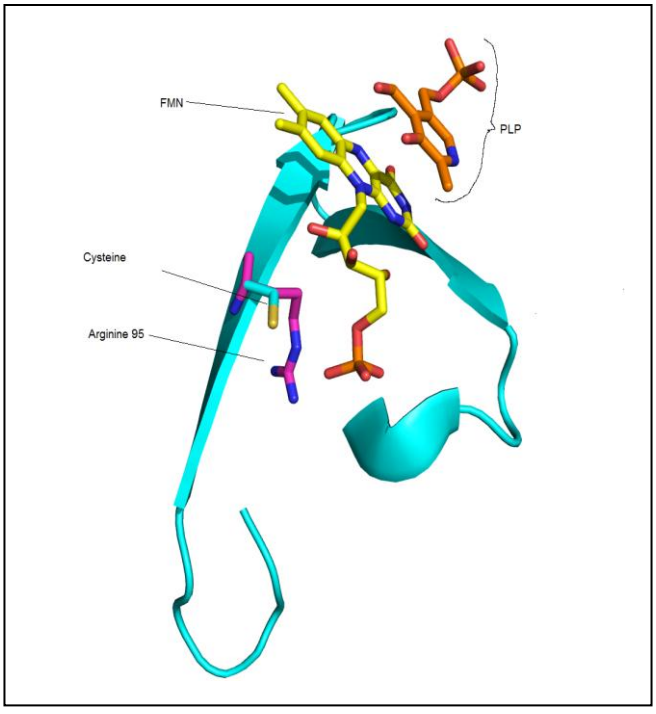


**Figure 11:** Active site structure of human PNPO Arg 95 mutated to Cys

To test our hypothesis and elucidate the reason behind the loss of catalytic activity in hPNPO R95C mutant we expressed and purified the mutant enzyme along with the wild type enzyme and performed the following experiments: (1) Kinetic activity assay; (2) FMN binding studies; (3) Secondary structure analysis; (4) Thermal stability analysis; (5) Structural studies using X-ray crystallography.

## 2.2 Materials and methods:

**A. Cloning and site directed mutagenesis of hPNPO cDNA:** The cDNA coding for wild type human PNPO (hPNPO) was inserted into the pET28a(+) expression vector by Fike *et al.*[16] pET28a(+) adds 20 residues to the N terminus of hPNPO. These include six His residues which help in purification of the protein by a Ni-NTA resin affinity chromatography. The cloning region of pET28a-c(+) is shown in Figure 12. The R95C mutant was made on the cDNA coding for the wild type enzyme. A standard protocol mentioned in *QuickChange* kit from Stratagene was followed for the mutagenesis. Wild type hPNPO plasmid was used as the template DNA. Primers synthesized by integrated DNA technologies were: Forward: 5'- GGA AAA CCC TCT GCT **TGC** ATG TTG CTG CTG AAG - 3' and reverse: 3'- CCT TTT GGG AGA CGA **ACG** TAC AAC GAC GAC TTC - 5'. The underlined nucleotides correspond to codon changes. The PCR reaction was set up using manufacturer's recommendations. The PCR product was transformed into chemically competent *E. coli* Rosetta (λDE3)pLysS cells (Novagen), where 50 µl of the chemically competent Rosetta cells stored at -80°C were thawed on ice for approximately 5 minutes and about 5 µl (~50 ng) of the plasmid was mixed with them. The mixture was incubated on ice for about 30 minutes. The cells were then subjected to heat shock in a water bath maintained at 42 °C for 75 seconds and the tube was transferred onto ice. The cells were allowed to grow in 250 µl SOC medium for one hour at 37 °C. The transformation mixture was plated on LB agar plates containing 50 µg/ml of Kanamycin (Fisher) and 34 µg/ml of Chloramphenicol (Fisher) and allowed to grow overnight at 37 °C. The recombinant plasmid was isolated from these cells by using QIAprep miniprep plasmid purification kit from Qiagen. Concentration of the plasmid was determined using $A_{260\ nm}$ on UV-Vis Spectrophotometer.

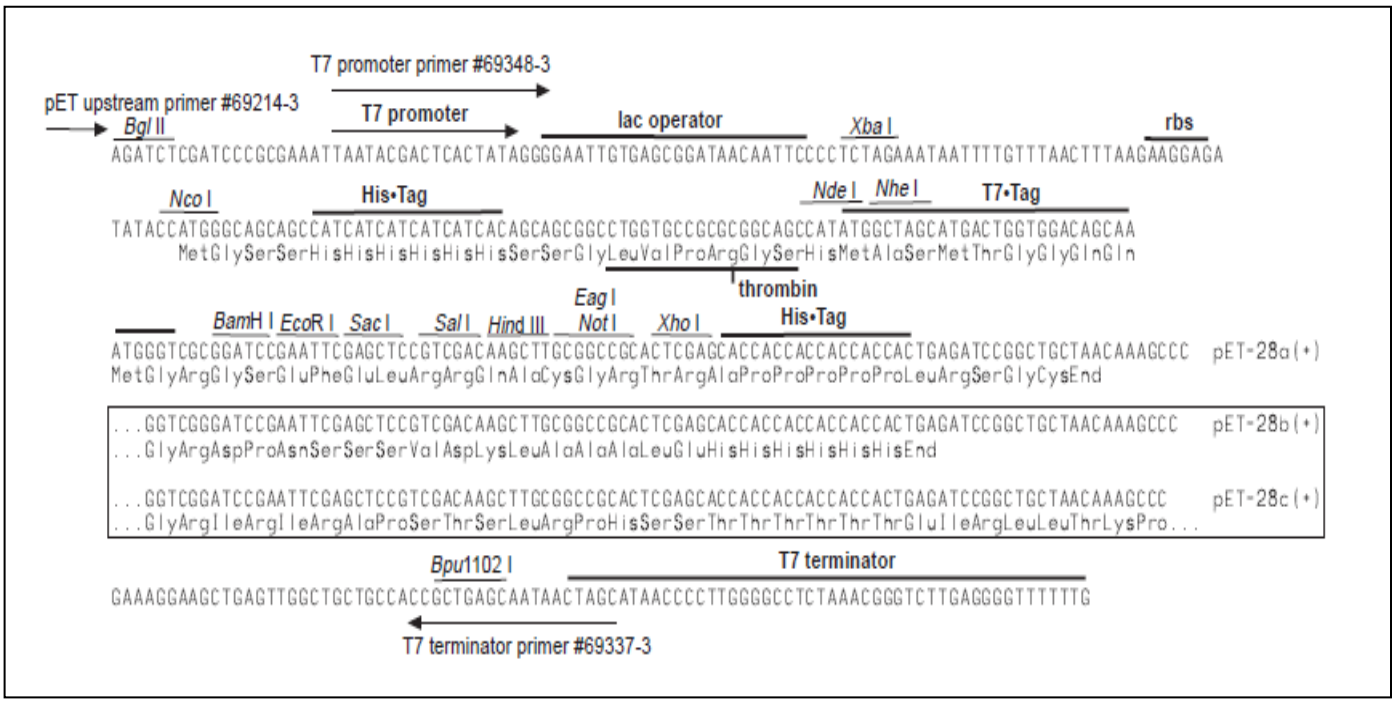


**Figure 12:** Cloning/expression region of pET28a-c(+)

**B. Expression and purification of R95C mutant:** A single colony from the plate containing the mutated recombinant pET28a(+) plasmid transformed in *Rosetta* cells, was used to inoculate 300 ml Luria Bertani (LB) medium containing Kanamycin (40µg/ml), Chloramphenicol (34 µg/ml), buffered to pH 7.2 with 100 mM potassium phosphate. This was incubated overnight at 37 °C, with shaking at the speed of 200 rpm and the overnight grown culture was used to inoculate 6 L of LB medium (similar composition as used before). Cells were grown at 37 °C with rotary shaking until the $OD_{600\ nm}$ reached 1.0 and then induced with IPTG (isopropyl β-D-thiogalactopyranoside) under two sets of conditions: (1) overnight induction with 50 µM IPTG at 18 °C and (2) induction for five hours with 0.5 mM IPTG at 37 °C. Cells were harvested by centrifugation at 5000 rpm for 15 minutes and resuspended in cold 50 mM potassium phosphate buffer at pH 7.4, containing 300 mM NaCl, 5 mM 2-mercaptoethanol and 10 µM FMN. Either 1 mM PMSF (phenyl methyl sulfonyl fluoride) or 2 ml protease inhibitor cocktail solution from Sigma was added to the cell lysis buffer as protease inhibitors. All the further purification procedures were carried out between 0-4°C. Lysis of the resuspended cells was carried out using a French press from Avestin at pressure exceeding 20,000 psi. The cell debris were separated from the suspension by centrifugation at 12,000 rpm for 20 minutes. The solubility of the mutant enzyme was determined by loading the soluble (supernatant) and insoluble (precipitate) fractions onto a 10% SDS PAGE.

200 mg of Streptomycin sulphate (Fisher) dissolved in 10 ml of cell lysis buffer was added with constant stirring to the supernatant and the solution was centrifuged to remove the DNA bound to streptomycin sulfate. A yellowish white precipitate was separated. The clarified protein solution was added onto a $Ni^{+2}$-nitrilotriacetic acid (Ni-NTA) column (QIAGEN) (3cm X 8 cm) pre-equilibrated with 50 mM potassium phosphate buffer (pH 7.4) containing 300 mM

NaCl, 5 mM 2-mercaptoethanol and 5 mM imidizole. The column was washed with the equilibration buffer until $A_{280\ nm}$ of the flow through was below 0.1. The mutant protein was eluted by gradually increasing the concentration of imidazole in the equilibration buffer to 150 mM. Fractions were analyzed by 10% SDS PAGE. *Precision Plus Protein Dual Color standard* from Biorad was used as the protein molecular weight standard. The pure fractions were pooled and dialysed against 50 mM potassium phosphate buffer (pH 7.4) containing 5 mM 2-mercaptoethanol. Concentration of the protein was determined by using molar extinction coefficient of 76,760 $cm^{-1}M^{-1}$ at 280 nm, which possesses an absorbance of 1.67 for 1 mg/ml solution.

**C. Cloning, expression and purification of hPNPO wild type:** The wild type was cloned in pET28a(+) as mentioned before and transformed in *E. coli* HMS174 cells, which require Kanamycin (50 µg/ml) for selection. The expression and purification procedure of the wild type was silimar to that of the mutant, using Ni-NTA affinity chromatography.

**D. Catalytic activity assay:** PNPO with the help of the cofactor, FMN oxidizes PNP or PMP to PLP as shown in Figure 4. The activities of the wild-type and R95C mutant enzymes were followed using PNP as the substrate. The assays were performed in a water-jacketed, 10 cm pathlength cuvette at 37 °C, in 50 mM Tris-HCl buffer at pH 8, containing 10 µM FMN. The reaction mixture also contained 1 mM dithiothreitol (DTT). The structure of Tris is shown in Figure 13. As the reaction proceeds the product PLP forms aldimine with the amino group of Tris in the buffer. This can be followed at 414 nm where the aldimine absorbs maximally with a molar absorbance coefficient of 5900 $cm^{-1}M^{-1}$. Kinetic constant measurements were carried out with fixed concentrations of both the enzymes (mutant and wild type). The substrate PNP concentrations were varied between 0.01 to 2 mM. Initial velocities were determined for the first 60 seconds of the reaction monitored at 414 nm. $K_m$ and $k_{cat}$ values were determined from the double reciprocal plots of the initial velocities and substrate PNP concentrations.

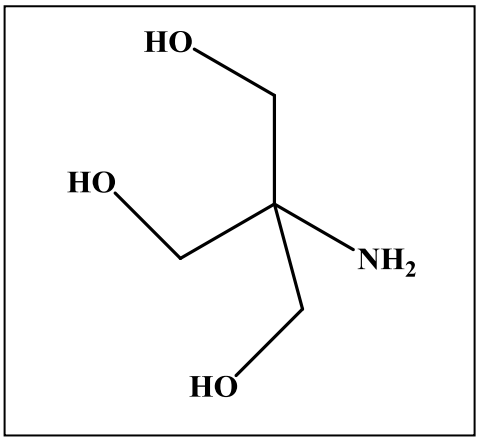


**Figure 13:** Structure of Tris(hydroxymethyl)aminomethane

**E. FMN binding study using fluorescence spectroscopy:** PNPO uses FMN (Figure 14) as a cofactor. Fluorescence of FMN is different in free and protein bound states. Quenching of FMN fluorescence upon binding to apo PNPO was followed to determine the dissociation constant ($K_d$) for FMN binding to the wild type and R95C mutant.

**Preparation of apoenzyme:** During the course of this study a number of procedures were tried to prepare apo PNPO. Initially the procedure described by Di Salvo *et al* was attempted which involved the use of phenyl sepharose column for the removal of FMN.[15, 25] Later a procedure descibed by Tsuge and co-workers, which is based on dialysis of the holo enzyme against 200 mM potassium acetate buffer at pH 5, containing 2-mercaptoethanol and 1 M potassium bromide for 12 hours was standardized and used for apo hPNPO preparation.[73]

**Determination of dissociation constant ($K_d$) of FMN binding to apo enzyme:** Apo PNPO sample (either wild type or R95C mutant) was added to 50 nM FMN in 50 mM potassium phosphate buffer (pH 7.2) containing 1 mM DTT. Excitation wavelength was set at 450 nm with excitation slit of 1 nm on a *Shimadzu RF-5301 PC*. Fluorescence emission spectra for FMN between 470 nm to 570 nm with 10 nm emission slit were recorded using 1 cm pathlength quartz cell. $K_d$ was calculated based on equation 1, where $\Delta F/F_0$ is the fractional fluorescence change at 525 nm at varying concentrations of apo enzyme, $\Delta F_{max}$ is the maximum change in fluorescence intensity, [APO] is the total apo enzyme concentration, [FMN] is the total cofactor concentration, $K_d$ is the dissociation constant of the equilibrium: APO + FMN ⟷ HOLO. The $K_d$ values were calculated by plotting $\Delta F/F_0$ against concentration of apoenzyme using *SigmaPlot 11.0*.

$$\frac{\Delta F}{F0} = \Delta F_{max} \times \frac{\text{APO} + \text{FMN} + Kd - \sqrt{(\text{APO} + \text{FMN} + Kd)^2 - (4 \times \text{FMN} \times \text{APO})}}{2 \times \text{FMN}} \quad \textbf{(1)}$$

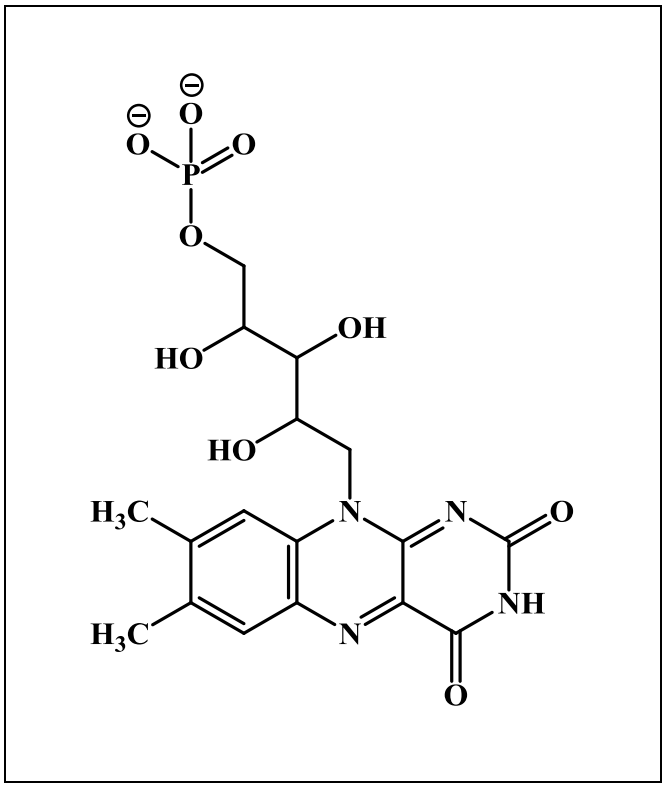


**Figure 14:** Structure of flavin mononucleotide (FMN)

**F. Secondary structure analysis using circular dichroism:** Circular dichroism (CD) spectroscopy is an excellent tool for rapid determination of secondary structure and folding characterics of proteins. We used the protein CD spectra to determine if the Arg95 to Cys mutation in PNPO has affected its conformation. Both wild type and R95C mutant PNPO were diluted in 50 mM sodium phosphate buffer, pH 7 to make 0.1 mg/ml solutions. CD spectra for both the samples were recorded on *Olis* optical spectropolarimeter at room tempertature using a 0.5 cm cell and the obtained spectra were converted to mean residue ellipticity (molar ellipticity) (Θ), which gives the CD signal per amino acid based on peptide concentration (c), path length of the cell (l) and mean residue weight (n) using equation 2.

**(2)**

$$\Theta = \Theta^{\circ} \times \frac{M}{c.l.n}$$

Where, $\Theta^{\circ}$ is the observed ellipticity in degrees and M is the molecular weight of the protein.

Mean residual weight (n) = $\frac{molecular\ weight\ of\ protein}{number\ of\ amino\ acids}$

**G. Thermal stability analysis:** The three amino acids responsible for intrinsic fluorescence of folded proteins are tryptophan, tyrosine and phenylalanine. The most dominant is tryptophan which is characterized by bicyclic conjugate system of indole moiety. Tryptophan has an absorbance maximum near 280 nm and an emission maximum which is environment sensitive. In a non polar environment, for example in hydrophobic core of proteins or in an organic solvent, Trp shows an emission maximum near 320 nm; whereas it shifts to near 350 nm in a polar environment, for example a solvent exposed Trp in proteins or when dissolved in aqueous solvents. Melting temperatures ($T_m$) of both wild type and R95C mutant of PNPO were determined by following the change in tryptophan fluorescence when heated from 20-70 °C and the thermal stabilities of both the proteins were compared. Melting temperature is the point on the melting curve of a protein where 50% of the protein has denatured.

Protein samples of wild type and mutant enzymes (3.5 µM) in 50 mM sodium Hepes buffer pH 7.2, containing 0.2 µM DTT and 0.1 µM EDTA, were heated from 20-70 °C with a heating rate of 5°C per minute using a circulating water bath. Fluorescence spectra of samples at all temperatures were recorded on fluorescence spectrophotometer by *Photon Technology International*. The excitation wavelength was set at 280 nm. Emission spectra were recorded from 300 to 380 nm with excitation slit of 2.5 nm and emission slit of 5 nm. The change in tryptophan fluorescence at 329 nm was noted and a melting curve was plotted. A derivative plot of the melting curve was then plotted to determine the melting temperature ($T_m$) of both the proteins.

**F. Structural determination by X-ray crystallography:** All the 100 crystallization conditions from *Hampton Research* were screened with the mutant enzyme. The protein concentration was varied from 7 mg/ml to 27 mg/ml. Purity of the protein was above 90% based on SDS PAGE analysis.

### 2.3 Results and discussion:

**A. Site directed mutagenesis, expression and purification of the R95C mutant:** Expression of the R95C mutant was generally low as observed on the SDS PAGE of the soluble (cell lysate) and insoluble (pellet) fractions as explained in Section 2.2.B. Overnight induction with 0.05 mM IPTG at 18 °C showed better expression compared to five hours induction with 0.5 mM IPTG at 37 °C (Figure 15). The pH of 7.2 of the LB medium was found to be critical for expression since no expression was observed in unbuffered medium. The mutant enzyme bound to the $Ni^{2+}$-NTA column as a yellow band and purification yielded ~90% pure protein as observed on SDS PAGE of the fractions collected from the column (Figure 16). The enzyme is yellow, although intensity of the color is less compared to the wild type. $A_{280\ nm}$ is the result of seven Trp residues and nine Tyr residues per subunit of the enzyme.

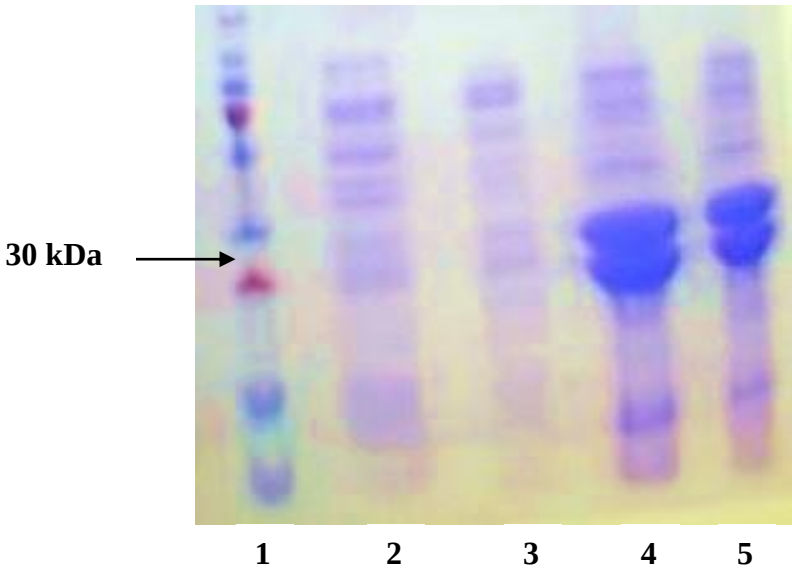


**Figure 15: SDS PAGE analysis of expression conditions attempted for R95C mutant:** (1) Marker; (2) Soluble, 18 °C 0.05 mM IPTG; (3) Soluble, 37 °C, 0.5 mM IPTG; (4) Insoluble, 18 °C, 0.05 mM IPTG; (5) Insoluble, 37 °C, 0.5 mM IPTG

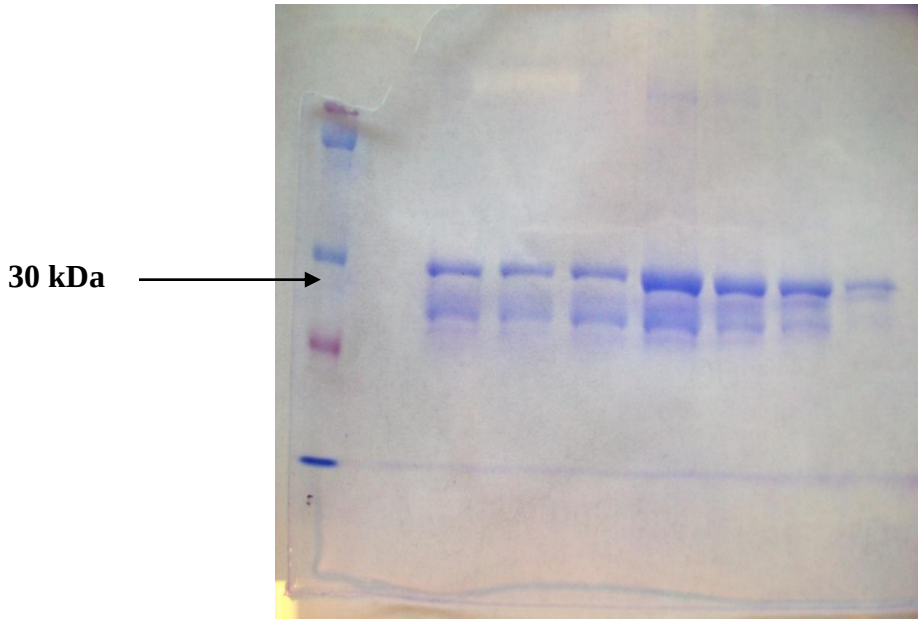


**Figure 16: SDS PAGE of purified hPNPO R95C:** Fractions collected after Ni-NTA column

More than one closely spaced band was seen on the SDS PAGE of the purified mutant enzyme. (Figure 16) Such multiple bands were previously reported with the wild type hPNPO.[16] Musayev *et al* analyzed amino acid sequences of these bands observed on SDS-PAGE of the wild type enzyme and showed protease digestion at the N-terminus to be the cause of such multiple molecular weight bands. The wild type enzyme has been crystallized with both the full length and truncated forms, and the two structures show similar fold.[16] With the mutant too, the enzyme preparation showed such multiple bands even though protease inhibitor was added before cell disruption and all the protein purification steps were carried out between 0-4 °C. The mutant protein samples stored at 4°C, -20°C and -80°C all showed degradation. The enzymes, wild type as well as the R95C mutant, when fresh showed lesser degradation which increased over the time. This, however, did not affect the catalytic activity of the enzyme.

**B. Expression and purification of wild type hPNPO[16]:** The wild type of PNPO cloned in *E. coli* HMS174 cells was expressed with similar induction conditions to that of the R95C mutant at 0.05 mM IPTG, overnight at 18 °C at 200 rpm. The protein was purified using $Ni^{2+}$-NTA column and 10% SDS PAGE showed more than a single band near 30 kDa, indicating proteolysis as explained in section 2.3.A (Figure 17). The protein was yellow in color and exhibited absorption maxima near 280 nm, 385 nm and 448 nm (Figure 18). The $A_{280\ nm}$ corresponds to Trp and Tyr residues whereas $A_{385\ nm}$ and $A_{448\ nm}$ correspond to the absorption by the FMN molecules, one per subunit.

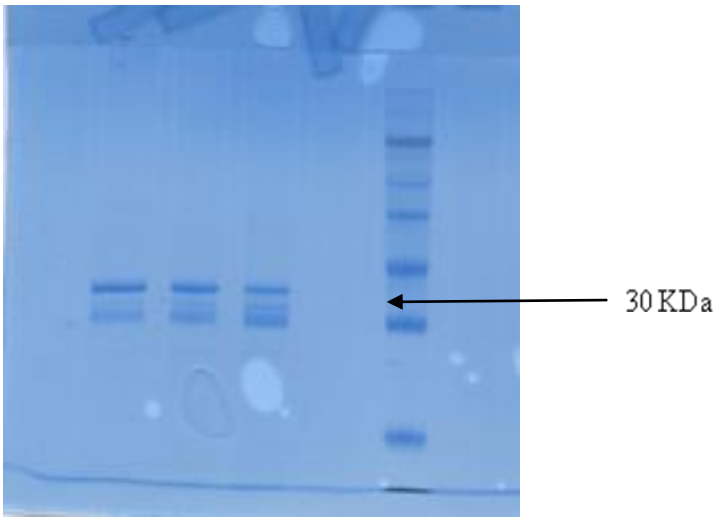


**Figure 17: SDS PAGE of purified hPNPO wild type:** Fractions collected after Ni-NTA column

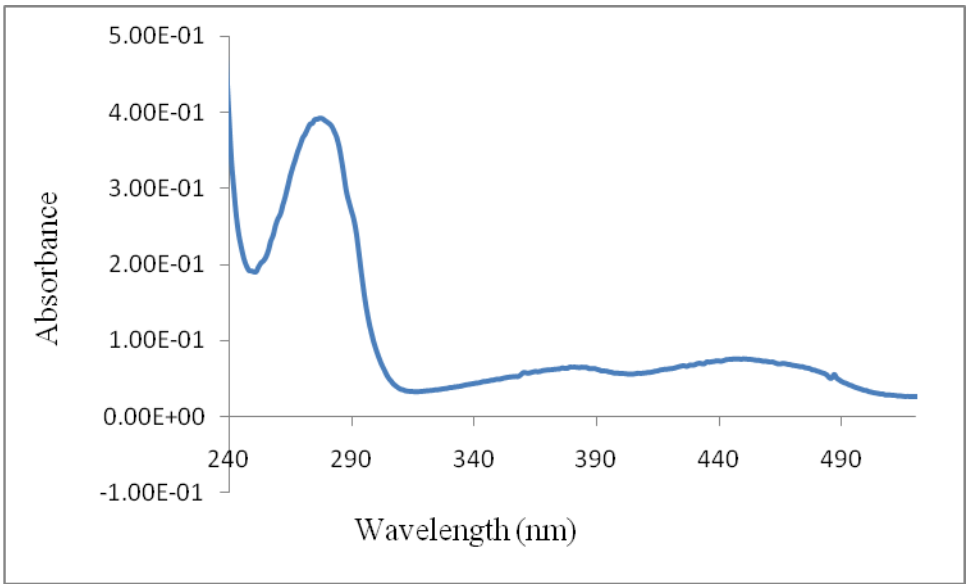


**Figure 18: UV-Vis spectrum of hPNPO wild type:** Protein exhibits peak at 280 nm whereas FMN exhibits peaks near 380 nm and 450 nm; the ratio of $A_{280}$:$A_{450}$ is near 7 for pure protein preparation

**C. Catalytic activity assay:** PNPO catalyzes the terminal step in the biosynthesis of PLP i.e. conversion of PNP or PMP to PLP. The human enzyme is sluggish with low turnover number, 0.19 $sec^{-1}$ for PNP and 0.20 $sec^{-1}$ for PMP. The enzyme has equal affinities for both the substrates unlike the *E. coli* enzyme which has more affinity for PNP than PMP[16]. Enzymatic activity measurements of wild type and R95C mutant enzymes were carried out by following the formation of aldimine-PLP complex at 414 nm as previously described and Lineweaver-Burk plots of initial rates against PNP concentrations were obtained to determine $K_m$ and $k_{cat}$ values (Table 2) (Figure 19.a and 19.b). For comparative purposes, the table also exhibits $K_m$ and $k_{cat}$ values for the PNPO R229W mutant as previously reported by Musayev *et al.*[69]

**Table 2:** Kinetic constants for human PNPO*

| | **Wild type** | **R95C** | **R229W[69]** |
|---|---|---|---|
| **$k_{cat}$ ($s^{-1}$)** | 0.18 ± 0.02 | 0.037 ± 0.01 | 0.04 ± 0.01 |
| **$K_m$ (µM)** | 6.18 ± 0.5 | 436 ± 35 | 461 ± 27 |
| **Catalytic efficiency ($\mu M^{-1}s^{-1}$)** | 0.0219 | 0.0000841 | 0.0000864 |

*Enzymatic activity was measured by following absorption of PLP-aldimine complex at 414 nm. Values are average of at least three measurements

About 4.8 fold decrease in $k_{cat}$ compared to the wild type was observed in case of the R95C mutant; whereas $K_m$ value increased ~70 fold in R95C mutant. The catalytic efficiency was determined from the $K_m$ and $k_{cat}$ values by using Equation 3.

$$\text{Catalytic efficiency} = \frac{kcat}{Km} \quad \textbf{(3)}$$

The kinetic studies clearly indicate significant loss in catalytic efficiency of the enzyme after Arg95 is mutated to Cys as indicated by ~341 fold decrease in the catalytic efficiency of the wild type enzyme.

**(a)**

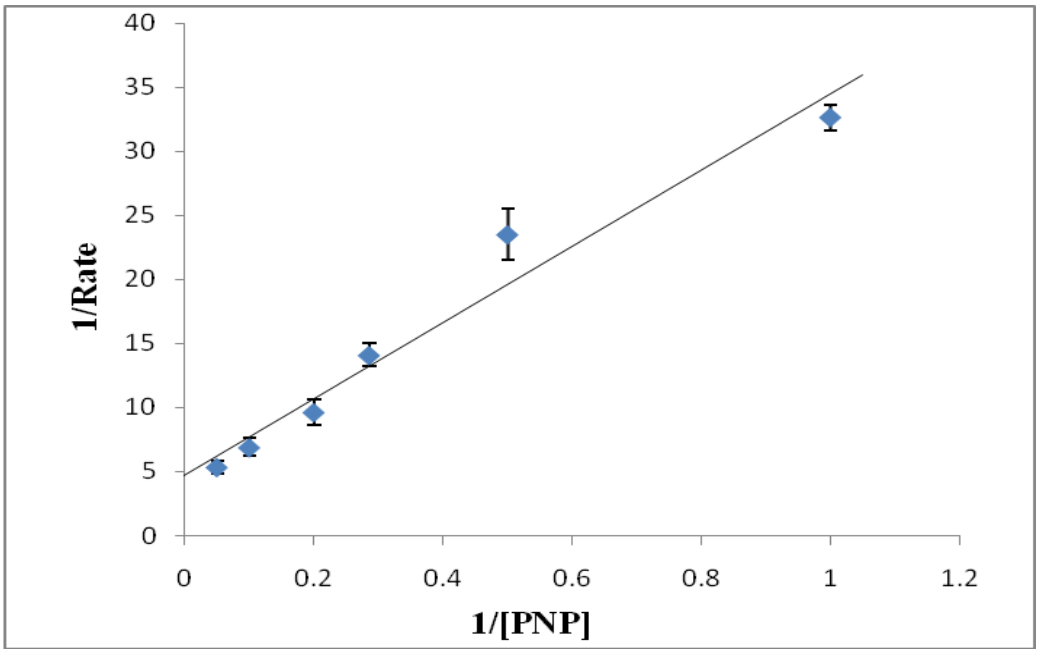


**(b)**

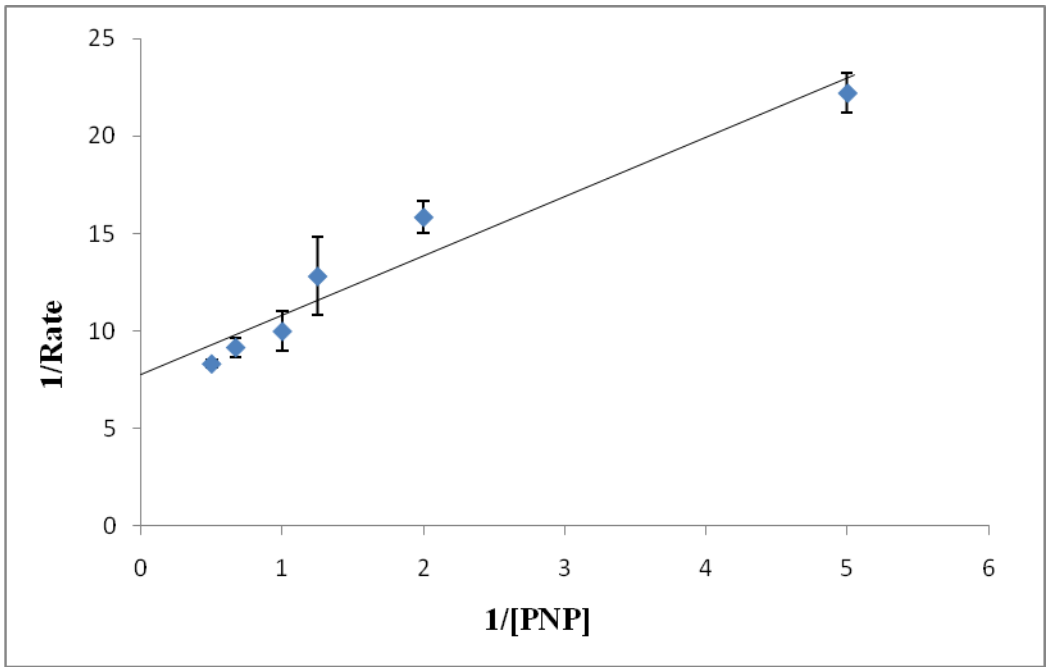


**Figure 19: Lineweaver-Burk plot representing the catalytic activity of hPNPO:** (a) Wild type; (b) R95C mutant

**D. FMN binding study using fluorescence spectroscopy:** The crystal structure of PNPO shows presence of cofactor FMN tightly bound in the active site of the enzyme by non-covalent interactions. (Figure 6) The substrate PNP or product PLP is present at the *re* face of FMN with close hydrophobic contacts between the two molecules.[16, 24, 69] FMN functions to remove electrons from the substrate. Arg 95 contributes to a highly conserved region of the active site of PNPO family and is observed to form salt bridge/hydrogen bond interactions with the phosphate side chain of FMN. The FMN binding studies were performed to determine if the loss of this interaction in case of R95C mutation, as well as change in the electrostatics of FMN phosphate binding site leads to attenuation of the affinity of FMN towards the enzyme, which may result in the loss of catalytic activity.

Fluorescence titration experiments were performed to determine the dissociation constant ($K_d$) of the FMN binding equilibrium. Quenching of FMN fluorescence was observed upon binding to apo enzyme of PNPO. Of several methods attempted for the preparation of apoenzyme, the first method involved passage of the protein through a phenyl sepharose column. However, separation of FMN from wild type enzyme was difficult using this method, due to high affinity of the cofactor towards wild type enzyme. This led to high dilution and decreased activity of the enzyme after reconstitution with FMN. The second method for the preparation of apoenzyme involved dialysis of the holo enzyme against buffer of low pH containing high salt. Preparation of apo enzyme was confirmed by disappearance of $A_{450\ nm}$ and $A_{380\ nm}$ peaks. This resulted in less dilution of the enzyme. About 90% catalytic activity of the enzyme could be recovered with this method after incubation with FMN (1:1). (Table 3)

**Table 3:** Initial rates of hPNPO catalytic activity assay (apo and holo comparison)

| | [PNP] | Holo ($min^{-1}$) * | Apo ($min^{-1}$)* | Apo Reconstituted ($min^{-1}$)* |
|---|---|---|---|---|
| **Wild type (10µM)** | 10 µM | 0.42 | 0.0267 | 0.39 |
| **R95C (10 µM)** | 2 mM | 0.3531 | 0.0012 | 0.34078 |

* Initial rates obtained by following absorption of aldimine formed between product PLP and Tris at 414 nm.

The fluorescence emission spectra of FMN after binding to increasing concentrations of apo enzymes of human PNPO are shown in Figure 20. The dissociation constants were determined for wild type and R95C mutant enzymes using Equation 1. (Table 4) The R95C mutant showed ~15-fold higher dissociation constant for FMN binding compared to the wild type enzyme, indicating low binding strength of the mutant for FMN. Dissociation constant of FMN towards apoenzyme of R229W mutant is shown in Table 5 for comparative purposes.

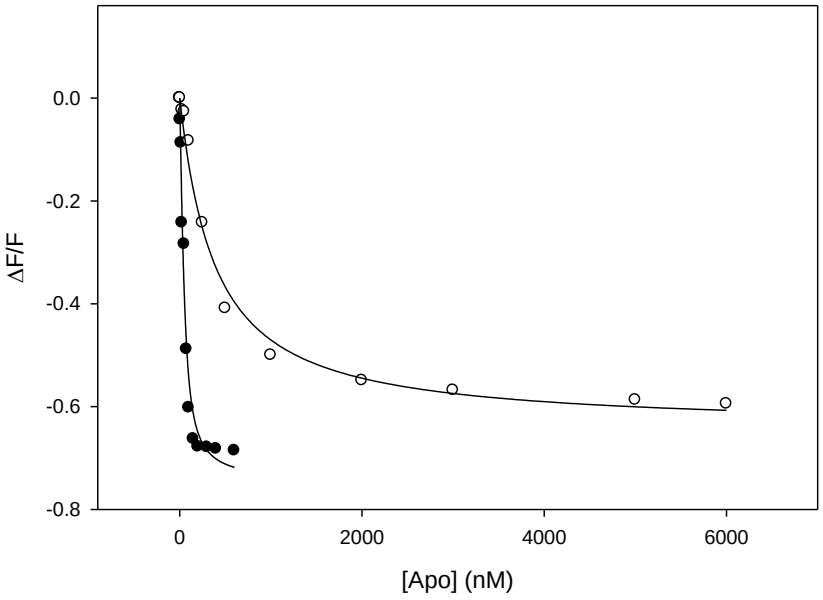


**Figure 20: Fluorescence emission spectra of FMN upon binding to apo hNPO:** Decrease in the relative FMN fluorescence emission intensity upon binding to apo forms of PNPO: wild type (●) and R95C mutant (○).

**Table 4:** Dissociation constants ($K_d$) for FMN binding to apo human PNPO

| **Protein** | **$K_d$ (nM)[a]** |
|---|---|
| Wild Type | 23.7 ± 3.2 |
| R95C | 354.3 ± 12 |
| R229W[b] | 672 ± 65 |

[a] $K_d$ is an average of at least 3 measurements

Lower $K_d$ values indicate higher affinity

[b] Reference 69

**E. Secondary structure analysis using circular dichroism:** The circular dichroic spectra were obtained for both the wild type and mutant enzyme preparations. There is no significant difference observed in the trends of the two proteins. (Figure 21) The mutation of Arg95 to Cys thus does not seem to have any significant effect on the secondary structure of human PNPO, even though affinity of the enzyme towards its cofactor FMN is diminished.

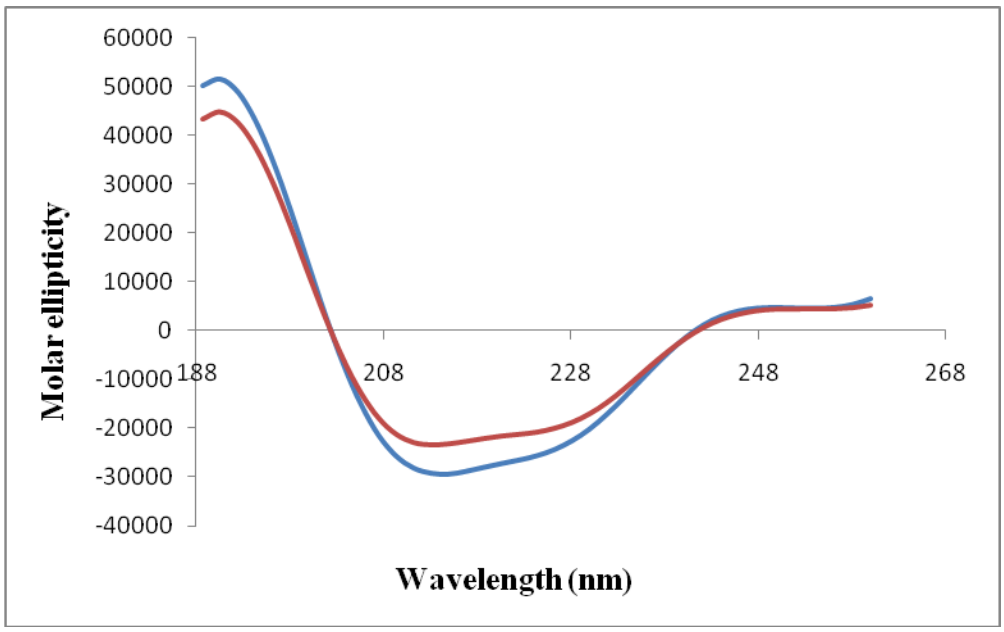


**Figure 21: Circular dichroism spectra of human PNPO:** Wild type (Red), R95C mutant (Blue)

**F. Thermal stability studies:** Thermal stability of the proteins was determined by heating the protein samples from 20-70 °C and following the quenching of Trp fluorescence. Figure 22 shows change in fluorescence of the wild type and R95C mutant of human PNPO with respect to the temperature change. Initially the peak maxima lie near 329 nm and 331nm which shift to 340 nm and 341 nm for wild type and R95C mutant respectively, as the protein denatures. The ability of the enzymes to refold was determined by cooling the proteins back to 20°C and collecting spectra at all stages. Figure 23.a and 23.b illustrate the changes in the fluorescence spectra before and after the thermal denaturation. The observed denaturations were irreversible for both the proteins. The change in fluorescence with varying temperatures was determined at 329 nm and melting temperatures ($T_m$) of the proteins were determined by plotting first derivative of the fluorescence intensity values as a function of temperature against increasing temperatures (Figure 24). There was no difference observed between the $T_m$ of both the proteins (64°C). This indicates that the thermal stability of both the enzymes is similar and the mutation of Arg95 to Cys has not affected the protein folding patterns of human PNPO.

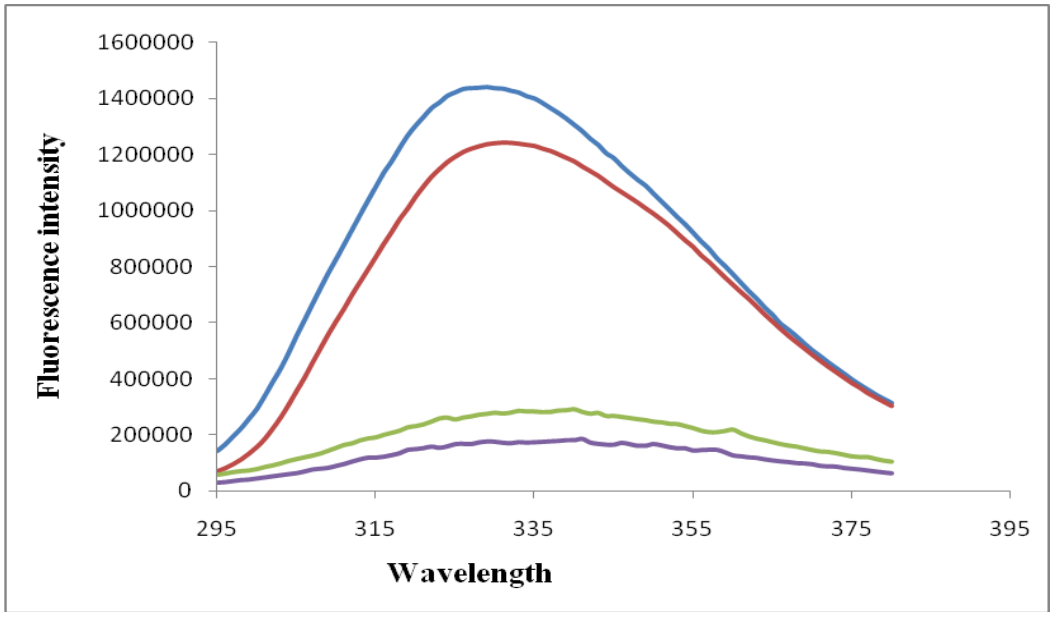


**Figure 22: Fluorescence spectral changes in human PNPO at increasing temperatures:** Wild type at 20°C (blue), R95C at 20°C (red), wild type at 70°C (green) and R95C at 70°C (purple)

**a**

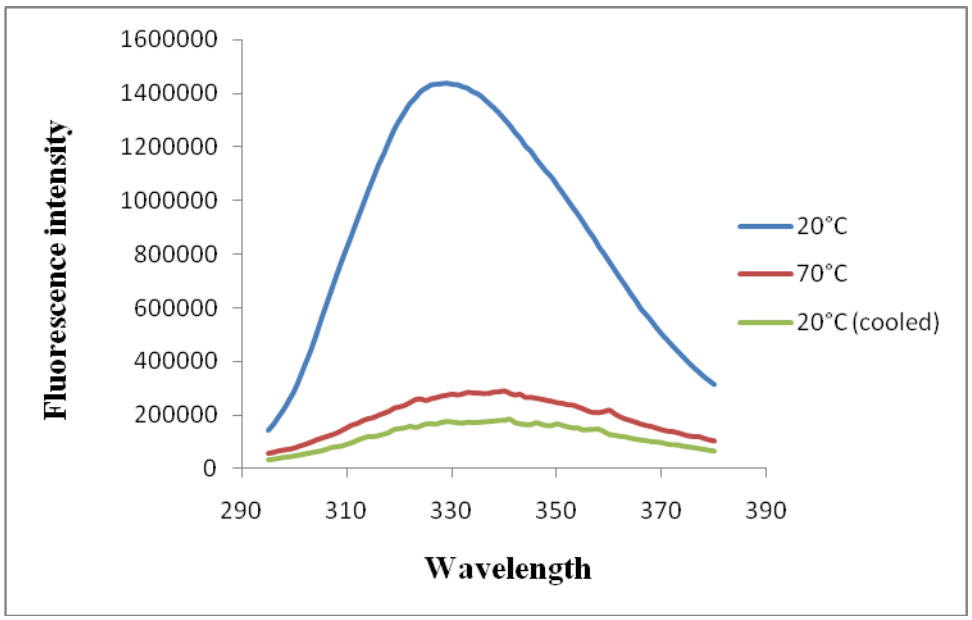


**b**

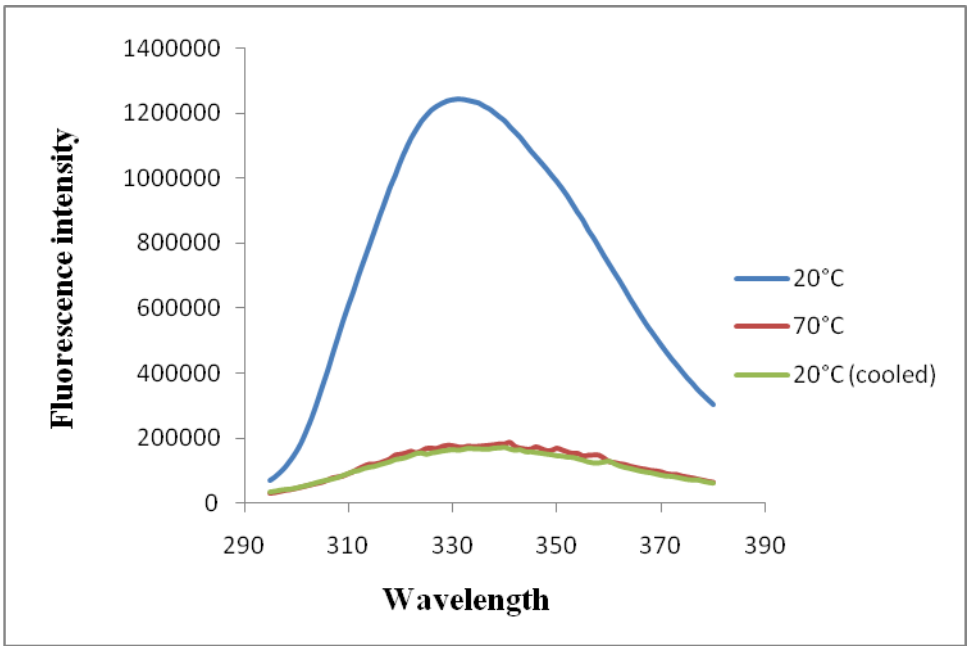


**Figure 23: Recovery of protein structure after heating and cooling of hPNPO: a:** wild type; **b:** R95C mutant; before heating at 20°C (blue), after heating at 70°C (red) and after cooling back to 20°C (green)

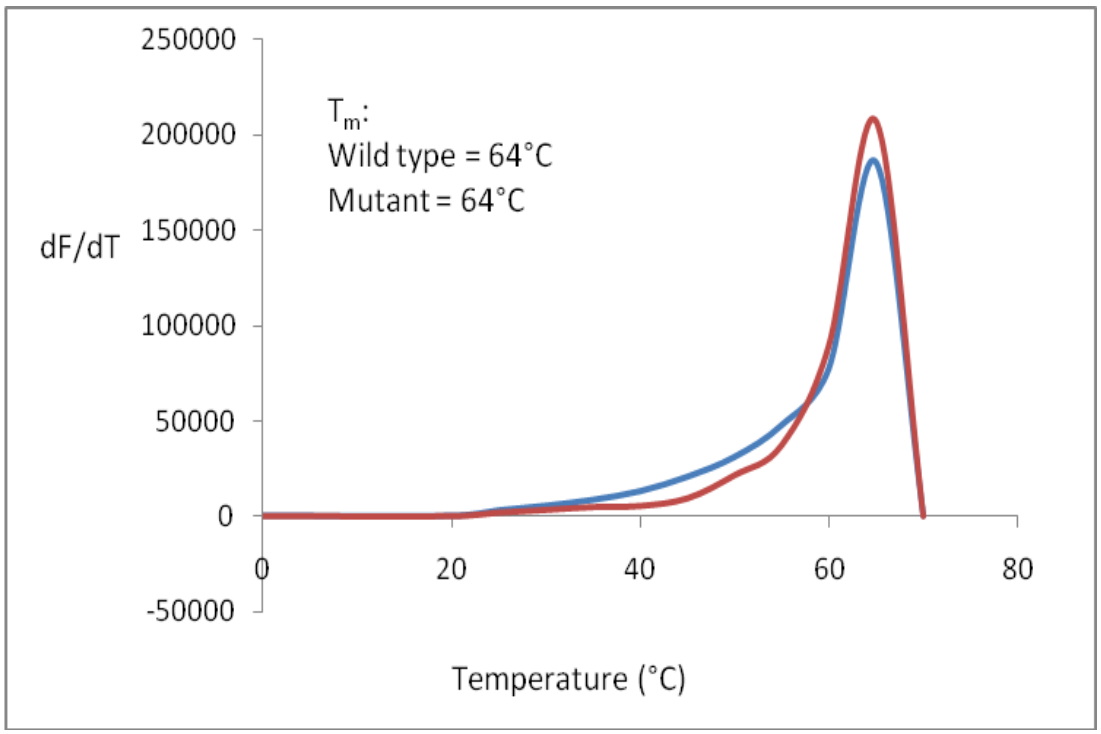


**Figure 24: Melting curve of human PNPO:** Wild type (blue) and R95C mutant (red)

**2.4 Conclusions:** A homozygous missense mutation of Arg95 to Cys in human PNPO is one of the several mutations associated with NEE. Our study with R95C was aimed at determining the molecular basis of the reduced catalytic activity of human PNPO exhibited by this mutant enzyme. Results indicate that the observed loss of catalytic efficiency of the enzyme is due to the reduced affinity of the mutant enzyme towards its cofactor FMN by about 15 fold. The diminished binding of FMN to the enzyme may be a result of the probable loss of hydrogen bonding interactions between Arg95 and the phosphate side chain of FMN, when the Arg residue is replaced by Cys. Similar conclusion was made for the PNPO R229W mutant, where replacement of Arg229 by Trp led to decreased affinity of FMN with a concomitant decrease in PLP production.[69] These observations clearly explain why the treatment of NEE with pyridoxine was unsuccessful in many cases because of inability of the PNPO to oxidize PNP or PMP to form PLP. The current treatment with PLP or PL is appropriate since the other enzyme involved in PLP metabolism, PLK, can convert PL to PLP. This study clearly shows that the PLP made *in vivo* from PL is not enough, indicating that PLK alone is not sufficient to meet the cell's requirements and both the salvage enzymes, PL kinase and PNPO, are necessary to provide PLP to activate over 140 different apo vitamin $B_6$ dependent enzymes.

Although we don't have crystallographic data, we speculate that the mutation may have also led to active site distortion which could decrease the enzyme binding affinity for PNP or PMP with a concomitant decrease in catalytic rate. This is consistent with the crystallographic structure of R229W mutant that showed significant distortion of the PNP binding site due to the mutation leading to reduced PNP binding affinity.

# Chapter 3

## Mechanism of transfer of pyridoxal 5'-phosphate from pyridoxine 5'-phophate oxidase to vitamin $B_6$ dependent enzymes

**3.1 Introduction:** PLP, a cofactor for many vitamin $B_6$ dependent enzymes is highly reactive owing to its aldehyde functionality. As a result the cell has devised several regulatory mechanisms that keep the concentration of free PLP very low. Nevertheless, apo PLP dependent enzymes manage to get enough supply of the cofactor. It is thus very intriguing to determine the mechanism by which the PLP produced by the salvage enzymes PNPO and PLK is transferred to the apo vitamin $B_6$ enzymes. There are two possible mechanisms for the transfer of PLP to apo B6 enzymes (Section 1.9). These include direct channeling from PNPO/PLK to apo B6 enzymes or release of PLP from PNPO/PLK into the solution in the cell which is then taken up by apo B6 enzymes. Our research is specially focussed on PNPO and this chapter consists of three individual but interrelated techniques used to determine the mechanism of PLP transfer from PNPO to vitamin $B_6$ dependent enzymes. These include affinity pull down and fluorescence polarization techniques to determine whether PNPO makes physical and specific interactions with B6 enzymes and the kinetic studies of PLP transfer from PNPO to apo-SHMT.

### 3.2 Materials and methods:

**3.2.A Expression and purification of proteins:** The proteins used to study the mechanism of PLP transfer included PNPO from human as well as *E. coli* as the enzyme involved in the biosynthesis of PLP. The vitamin $B_6$ dependent enzymes that were used include serine hydroxymethyl transferase (SHMT) from rabbit and *E. coli* and *E. coli* aspartate aminotransferase (eAAT). The enzymes were expressed, purified and prepared as previously reported, with some modifications.[15, 16, 64, 74, 75]

**(a) Human PNPO:** The enzyme was expressed and purified as outlined in Section 2.2.C.[16]

**(b) *E. coli* PNPO:** The protocol for the expression and purification of the dimeric *E. coli* PNPO (M.W. ~50 kDa) has been reported by Di Salvo *et al*[15]. The gene was cloned in pET22b(+) vector (Novagen) which was transformed in *E. coli* HMS174(DE3) strain (Novagen). The cells were expressed in YT (Yeast, Tryptone) medium containing 100 µg/ml of ampicillin and induced at 0.5 mM IPTG with shaking at 30°C for 5 hours. The cells were then harvested by centrifugation and lysed in 50 mM Tris buffer, pH 8 containing 2 mM EDTA using Avestin cell disrupter. The lysed cells were subjected to ammonium sulfate precipitation (25% followed by 55%) and dialysed against 20 mM potassium phosphate buffer, pH 6.8, containing 5 mM 2-mercaptoethanol and 0.2 mM EDTA to remove salt. The protein solution was then loaded on Sephadex CM-50 column (2.5 X 11 cm) preequilibrated with the dialysis buffer. Wash buffer was same as the equilibration (or dialysis) buffer and the column was washed until $A_{280\ nm}$ of the eluate was below 0.2. The protein was eluted from the column as a yellow band using a linear gradient of 100 ml equilibration buffer and 100 ml of 20 mM potassium phosphate buffer (pH

6.8) containing 400 mM NaCl, 5 mM 2-mercaptoethanol and 0.2 mM EDTA. The protein was then concentrated by 60% ammonium sulfate, desalted by dialysis and loaded onto a ceramic hydroxylapatite column (2.5 X 7.5 cm) preequilibrated with 50 mM potassium phosphate of pH 6.8 containing 5 mM 2-mercaptoethanol and 0.2 mM EDTA, for further purification. The protein was eluted using a linear gradient of equilibration buffer and 400 mM potassium phosphate buffer pH 6.8 containing 5 mM 2-mercaptoethanol and 0.2 mM EDTA. The protein purity was assessed using 10% SDS PAGE and was stored at -80°C with 10% glycerol.

**Activity assay:** The enzyme was assayed by following the formation of Tris-PLP aldimine complex at 414 nm as described in Section 2.3.C.

**(c) SHMT from rabbit liver cytosol:** SHMT belongs to Fold type I of the vitamin $B_6$ dependent enzymes. The rabbit liver enzyme is a tetramer with molecular weight of 52 kDa per monomer. The expression and purification protocol for rcSHMT has been reported previously by Di Salvo *et al.*[74] Gene coding for SHMT cloned in pET22b(+), was transformed into *E. coli* HMS174(DE3) cells. A single colony of the cells was used to inoculate 100 ml of LB medium containing 100 µg/ml of ampicillin. The inoculated medium was allowed to grow overnight at 37°C with shaking and was then used to inoculate 6 litres of LB medium buffered to pH 7.3 containing 100 µg/ml of ampicillin. The bacteria were allowed to grow at 37°C with shaking and after the $OD_{600\ nm}$ reached near 1.8, IPTG was added to the final concentration of 0.5 mM and aeration continued for another 4 hours. The cells were harvested by centrifugation at 5000 rpm for 15 minutes. The cell pellet was resuspended in 20 mM potassium phosphate buffer, pH 7.3, containing 0.1 mM PLP, 5 mM 2-mercaptoethanol and 0.1 mM EDTA. The cells were lysed using Avestin cell disrupter and the debris was removed by centrifugation at 12,000 rpm for 25 minutes at 4°C. Ammonium sulfate was then added to the supernatent to 55% saturation. The

precipitated protein was redissolved in 20 mM potassium phosphate buffer, pH 7.3 containing PLP, 2-mercaptoethanol and EDTA as described above and dialysed against the same buffer to remove ammonium sulfate.

The protein solution was loaded onto a Sephadex CM-50 column (8 X 15 cm) equilibrated with the dialysis buffer of pH 6.8. The protein was bound at the top of the column as a yellow band. The column was washed with the equilibration buffer until $A_{280\ nm}$ reached below 0.2. A linear gradient of the equilibration buffer and 300 mM potassium phosphate buffer, pH 7.3 containing 2-mercaptoethanol and EDTA was used for elution. The enzyme was eluted near the end of the gradient and those fractions showing $A_{278\ nm}/A_{428\ nm}$ near 7 were pooled together. The protein was then precipitated by ammonium sulfate to 60% saturation and redissolved in 20 mM potassium phosphate buffer, pH 7.3 containing 0.1 mM PLP, 5 mM 2-mercaptoethanol and 0.1 mM EDTA. The protein solution was dialysed against the same buffer without PLP.

The dialysed enzyme was loaded onto a column of ceramic hydroxylapatite (5 X 7 cm) equilibrated with 20 mM potassium phosphate buffer, pH 7.3, containing 5 mM 2-mercaptoethanol. The column was washed with the equilibration buffer until the $A_{280\ nm}$ of the flow through was below 0.1. Elution was done with a linear gradient of equilibration buffer and 300 mM potassium phosphate buffer, pH 7.3, containing 0.1 mM PLP and 5 mM 2-mercaptoethanol. The collected fractions having $A_{280}/A_{260}$ ratio more than 7 were pooled together. The protein was concentrated by 60% ammonium sulfate precipitation followed by dialysis against 20 mM potassium phosphate buffer, pH 7.3, containing 5 mM 2-mercaptoethanol and 0.05 mM PLP. Protein purity was assessed using 10% SDS PAGE. Concentration of the protein was determined by measuring $A_{280\ nm}$ (1 mg/ml solution of the protein giving absorbance of 0.72).

**Activity assay:** SHMT has many substrates such as serine, glycine and allothreonine, of which, allothreonine was used as a substrate to asses the catalytic activity of the enzyme. Acetaldehyde is the product of action of SHMT on allothreonine. This acetaldehyde, in presence of excess of alcohol dehydrogenase and NADH is converted to ethanol with subsequent oxidation of NADH to form NAD. $A_{340\ nm}$ was followed where NADH absorbs and which gradually reduces when NADH is consumed as the reaction proceeds.[74]

**(d) SHMT from *E. coli*:**[75] pBR322 plasmid containing *glyA* gene coding for SHMT (monomeric M.W. 45 kDa) was transformed into *E. coli* GS245 cells. A single colony from LB agar plate containing 100 µg/ml of ampicillin was incubated into LB medium containing 100 µg/ml ampicillin and grown overnight at 37 °C with shaking. This culture was then used to inocluate 6 litres of LB medium buffered to pH 7.4 containing 100 µg/ml ampicillin and 0.4% glucose. The cells were allowed to grow at 37°C with vigorous shaking until $OD_{600\ nm}$ reached near 1. The bacterial cells were then harvested by centrifugation at 13,000 rpm for 15 minutes. The pelleted cells were resuspended in 10 mM Tris HCl buffer, pH 8 containing 1 mM EDTA and cell lysis was carried out in Avestin cell disrupter. The protein was subjected to ammonium sulfate precipitation (50% followed by 75%) and the protein pellet obtained was dialysed against 20 mM potassium phosphate buffer pH 7.2, containing 0.1 mM PLP and 1 mM EDTA. The protein solution was then loaded onto a DEAE-Sephadex column (12 X 18 cm) pre-equilibrated with 20 mM potassium phosphate buffer pH 7.2 containing 0.1 mM PLP and 1 mM EDTA. The column was washed with the equilibration buffer until $A_{280\ nm}$ of the flow through was below 0.2, after which the protein was the eluted with a linear gradient of equilibration buffer and 20 mM potassium phosphate buffer, pH 6.4 containing 300 mM NaCl. The enzyme moved down as a yellow band and the fractions containing activity were pooled together. After 75% ammonium

sulfate precipitation, the protein pellet was dialysed against against 20 mM BES buffer, pH 7 containing 0.1 mM PLP.

This was followed by purifying the protein further using a 5 X 6 cm hydroxylapatite column. 20 mM BES, pH 7 was used as the equilibration and wash buffer. The enzyme was eluted using a linear gradient of the equilibration buffer and 100 mM potassium phosphate buffer, pH 7. The protein was then loaded onto a TMAE column for further purification if necessary. Enzyme purity was assessed using 10% SDS PAGE of the fractions collected after the final column.

**Activity assay**: Assay procedure was similar to rabbit SHMT, using allothreonine as a substrate.

**(e) Pyridoxal phosphatase from human brain:**[62] PLP phosphatase (M. W. 64 kDa) was cloned on the expression vector pET-19b and transformed into *E. coli Rosetta* (DE3) pLysS cells. The transformants were grown at 37 °C overnight in 200 ml LB medium with 100 µg/ml chloramphenicol and 100 µg/ml kanamycin. This grown culture was used to inoculate 6 L LB medium containing 100 µg/ml chloramphenicol and 100 µg/ml kanamycin and was grown to $A_{600\ nm}$ of 0.6. Induction was carried out overnight with 0.05 mM IPTG at 18 °C. The cells were harvested, washed and resuspended in 50 mM sodium phosphate buffer, pH 8, containing 300 mM NaCl and 5 mM imidazole and lysed using Avestin cell disrupter. Lysate was cleared by centrifugation at 12,000 rpm at 4 °C for 15 minutes. The supernatent was loaded on Ni-NTA column pre-equilibrated with 50 mM sodium phosphate buffer, pH 8, containing 5 mM imidazole. Elution buffer contained 50 mM imidazole in 50 mM sodium phosphate buffer, pH 8. Purity of the eluted protein was assessed using 10% SDS PAGE.

**Activity assay:**[62, 80] The assay of PLP- phosphatse activity was carried out in 1 cm thermostated cuvette in *Agilent 8454* spectrophotometer at $37^0$C by following decrease in $OD_{388\ nm}$, which indicates dephosphoryalation PLP to PL. PLP-phosphatse (about 20 µg) was taken in 20 mM sodium BES buffer, pH 7 containing 4 mM $MgCl_2$. The reaction was started by addition of the substrate PLP at concentration of 100 µM and decrease in OD at 388 nm was recorded for 60 seconds.

### 3.2.B Methods used to determine the mechanism of transfer of PLP from PNPO to vitamin $B_6$ dependent enzymes:

#### (a) Affinity pull down assay

Pull down assay is a qualitative *in vitro* method often used to determine physical interactions between proteins. Usually one of the proteins is tagged (called as bait) and the second one is called as the prey protein which is untagged. In a typical pull down assay the tagged bait protein is captured on an immobilized affinity ligand specific for the tag. The prey protein, either alone or in a cell lysate with other proteins, is then allowed to pass through the ligand bound bait protein. The unbound protein is washed and the complex between bait and prey protein (the protein-protein interaction) is eluted. Pull down assays are employed for purposes such as to confirm a previously suspected interaction between two proteins in which case the prey protein is expressed in an artificial protein expression system and is passed alone from the affinity ligand bound with the bait protein. On the other hand these assays could be used to discover unknown interactions between proteins.

The proteins of our interest are human PNPO and the Fold type I vitamin $B_6$ dependent enzyme, SHMT from rabbit liver cytosol. Human PNPO was used as the bait protein. The protein has six His residues at the N-terminus and therefore we used Ni-NTA as the affinity ligand. SHMT on the other hand has no tag and thus became the prey protein. The two proteins were mixed in equimolar concentrations (200 µM) to make about 200 µl of reaction mixture. The reaction mixture was incubated on ice for about 5 minutes. Approximately 500 µl of Ni-NTA slurry was packed on a column (0.5 X 1 cm) and equilibrated with 50 mM potassium phosphate buffer (pH 7.4) containing 5 mM imidazole, 5 mM 2-mercaptoethanol and 300 mM NaCl. The

protein mixture was loaded on the column slowly, which bound as a yellow band. The column was washed with the equilibration buffer until the $A_{280\ nm}$ of the flow through was below 0.2. Equilibration buffer containing 150 mM imidazole was used as the elution buffer. Both the enzymes, human PNPO and rc SHMT were subjected to the same procedure individually, to serve as controls. As another control, the experiment was carried out with a mixture of human PNPO and a non-vitamin $B_6$ dependent and non-His tagged protein, lysozyme. The flow through and eluates in all the above mentioned sets of experiments were collected and anaylsed using SDS PAGE.

### (b) Determination of $K_d$ by fluorescence polarization

Fluorescence polarization (FP) measurements have been used in analytical and clinical chemistry and as a biomedical research tool for studying membrane mobility, domain motions in proteins and interactions at molecular level. Several FP based immunoassays are used in clincal chemistry.[76]

When a small fluorescent molecule, called as tracer or ligand, is excited with plane polarized light, the emitted light is highly depolarized, due to tumbling of the tracer molecule. If the tracer is bound by a larger molecule its effective motion decreases and due to this reduced tumbling, the emitted light becomes more polarized (Figure 25). A fluorescence polarization instrument measures the binding interactions between proteins by monitoring changes in the size of the fluorescently labelled or inherently fluorescent molecules. We employed the technique to study and quantify the molecular binding interactions between PNPO and some vitamin $B_6$ dependent enzymes, including rabbit SHMT (rSHMT), *E. coli* SHMT (eSHMT) and *E. coli* aspartate aminotransferase (eAAT).

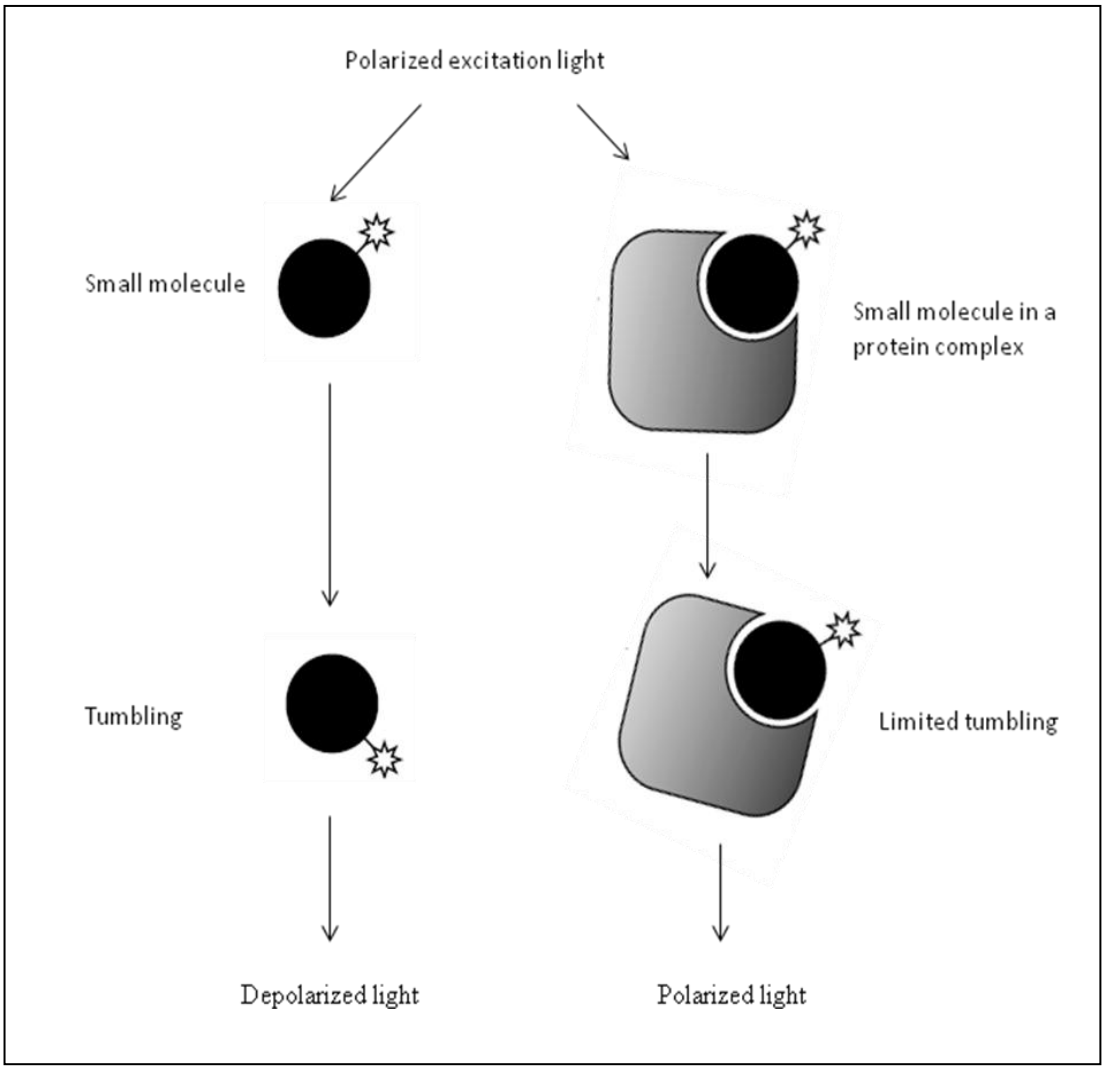


**Figure 25:** Principle of fluorescence polarization

**Labelling of human PNPO:** Human PNPO was selected as the molecule to be tagged and fluorescein 5-maleimide (FMi) (Invitrogen) was used as the fluorescent tag (Figure 26). FMi is a fluorescent molecule that reacts predominantly with sulfyhdryls at pH between 6.5 to 7.5 forming stable thioether bonds. Since PNPO does not have any sylfhydryl residues at the active

site, tagging with FMi does not hamper its catalytic activity. 50 µM human PNPO was mixed with 1 mM FMi in 1 ml of 50 mM sodium HEPES buffer, pH 7.55 containing 150 mM KCl and 0.01% Triton. The reaction was allowed to occur overnight at 4 °C in the dark. The reaction mixture was then centrifuged and the supernatant dialyzed against the same buffer in dark overnight to remove the excess dye. The tagged protein was stored at -20°C in amber colored container when not in use. The degree of labelling was determined by using equation 4. Catalytic activity of the protein was assessed before and after labelling by the assay procedure explained in section 2.2.D, to determine if labelling interferes with the activity of human PNPO.

$$\text{Moles fluor per mole protein} = \frac{A_{max} \text{ of the labeled protein}}{\varepsilon' \times \text{protein concentration (M)}} \times \text{dilution factor}$$

$A_{max}$ is $A_{495\,nm}$ and ε' is the molar extinction coefficient of FMi, which is 68,000 $M^{-1}$ $cm^{-1}$.

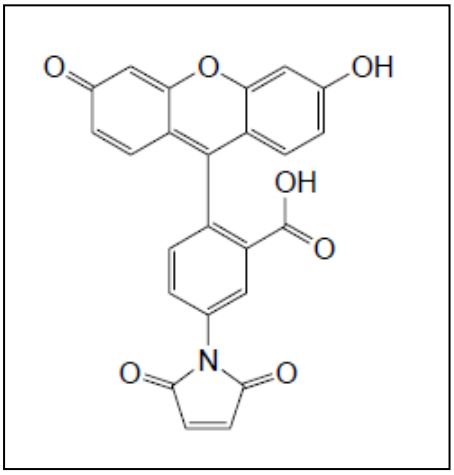


**Figure 26:** Fluorescein maleimide

**Preparation of enzyme solution:** The vitamin $B_6$ enzymes and controls were dialyzed against 50 mM sodium HEPES buffer, pH 7.55 containing 150 mM KCl and 0.01% Triton (100 X) overnight at 4 °C prior to use.

**Fluorescence polarization assay:** The assay was performed using *Tecan Polarion*. The excitation wavelength was set at 495 nm and emission wavelength at 535 nm. 0.1 µM of tagged human PNPO was added to separate wells in a 96 well round bottom polystyrene opaque plate Model # 3792 by *Corning Inc*. The vitamin $B_6$ dependent enzymes were added to the wells at concentrations ranging from 0-20 µM. The plate was incubated at 25 °C. Fluorescence polarization of the protein mixtures in all the wells was determined at every 5 minutes interval for up to 60 minutes. The polarization values were obtained by using *Microsoft Excel* interfaced with the polarimeter. The polarization values in mP were plotted against varying concentrations of vitamin $B_6$ dependent enzymes. Binding data between human PNPO and vitamin $B_6$ dependent enzymes was fitted and analyzed using *SigmaPlot 11*. $K_d$ value calculations were determined based on the principle that the measured polarization signal in mP is a weighted sum of the free ligand signal and bound ligand signal using equation 5

$$P_{obs} = \frac{([FMI-PNPO]P_{FMI-PNPO} + [FMI-PNPO-E]P_{FMI-PNPO-E})}{([FMI-PNPO] + [FMI-PNPO-E])} \qquad \textbf{(5)}$$

Where, $P_{obs}$ stands for the observed polarization value; $P_{FMI\text{-}PNPO}$ is the polarization value of tagged PNPO; $P_{FMI\text{-}PNPO\text{-}E}$ is the polarization value of tagged PNPO with PLP-dependent enzyme, when all the PNPO was in the complexed form; [FMI-PNPO] and [FMI-PNPO-E] are the concentrations of uncomplexed and complexed tagged PNPO respectively.

The equation to determine $K_d$ (Equation 6) was obtained from equation 5 by assuming that,

**FMi-PNPO + E ⟷ FMi-PNPO-E.**

$$P_{obs} = \frac{(P_0 * K_d + 2P_{max} * [E])}{(K_d + 2[E])} \quad \textbf{(6)}$$

$P_{obs}$ is the observed polarization value; $P_0$ is the polarization value in the absence of $B_6$ dependent enzymes; $P_{max}$ is the maximum polarization value obtained upon addition of $B_6$ dependent enzymes; $K_d$ is the dissociation constant of the interaction between the proteins (an indicator of affinity between the proteins) and [E] is the concentration of $B_6$ dependent enzymes.

As a control, binding curves of non-vitamin $B_6$ dependent enzymes, lactate dehydrogenase (LDH) and lysozyme with human PNPO were also obtained.

### (c) Kinetic studies of PLP transfer

SHMT catalyses many biochemical reactions as mentioned in Section 3.2.2, one of which is conversion of glycine to serine, where tetrahydrofolate (THF) serves as a co-substrate and functions as a 1-C carrier. In this reaction the PLP bound to SHMT forms a quinonoid complex with glycine and THF that absorbs between 490 to 495 nm.[77-79] We used this property of the ternary complex formed between enzyme bound PLP, glycine and THF to determine the kinetic profile of addition of PLP from a complex of PNPO-PLP to apo SHMT.

**Preparation of PNPO-PLP complex:** PNPO from human as well as *E. coli* was used for this experiment. Both the enzymes were prepared freshly by the procedure mentioned in Sections 2.2.C and 3.2.B respectively. PLP was obtained from Sigma. 300 µM of PNPO was mixed with 900 µM PLP. The ratio of 1:3 for PNPO:PLP was always maintained while preparing the complex. The mixture was incubated at 25°C for 30 minutes and the excess PLP was removed by dialysing the mixture overnight at 4°C against 50 mM sodium BES buffer, pH 7 containing 5 mM 2-mercaptoethanol, with two buffer changes. After dialysis the mixture was loaded on a gel filtration column of Sephadex G50 (0.6 X 45 cm), pre-equilibrated with 20 mM sodium BES buffer pH 7, containing 5 mM 2-mercaptoethanol. The complex mixture bound to the column as a dark yellow band. The column was then washed with equilibration buffer to elute the complex free from any unbound PLP.

**Determination of stoichiometry of PLP binding to PNPO:** Two methods were employed for the determination of stoichiometry of PLP binding to PNPO. In the first method, PNPO (15 µM) complexed with PLP was diluted 10 times in 50 mM sodium BES buffer pH 7, to the final volume of 1000 µl. NaOH was added to the diluted complex to the final concentration

of 0.1 M in order to inactivate the enzyme and release the bound PLP. The concentration of the released PLP was determined using molar extinction coefficient of 6600 $M^{-1}cm^{-1}$ and it was compared to concentration of the protein. The second method involved determining concentration of PLP released from PNPO, based on the activation of apo-SHMT to holo-SHMT, and comparing it with the concentration of PNPO determined by $A_{280\ nm}$. This method took advantage of a unique absorption maximum at 491 nm upon formation of an abortive ternary complex of holo-SHMT, glycine and THF, as explained earlier. 30 µM of apo-eSHMT was titrated with varying concentrations of free PLP at 37 °C in presence of glycine (50 mM) and THF (100 µM) in 50 mM sodium BES buffer, pH 7. A linear standard plot of $A_{491\ nm}$ versus concentration of free PLP was obtained based on the activation of apo-eSHMT. Freshly prepared complexes of human and *E. coli* PNPO-PLP (30 µM, based on $A_{280\ nm}$) were diluted 5-fold into 0.1 M NaOH, which denatured the enzyme under basic conditions and released bound PLP. 350 µl of 100 mM sodium BES of pH 6.5 was added to the protein mixture, to neutralize the pH. Activation of 30 µM apo-eSHMT was carried out with this reaction mixture in presence of glycine and THF in 50 mM sodium BES buffer, pH 7. The concentration of released PLP was calculated by extrapolating from the final absorbance at 491 nm, using the linear standard plot and compared to the concentration of PNPO.

**Catalytic activities of PNPO and PNPO-PLP complex:** The enzymatic activities of 200 µg of both human and *E. coli* enzymes were measured as per the procedure mentioned in Section 2.3.C, where formation of aldimine between product PLP and Tris in the buffer was followed at 414 nm.[15] 200 µg of both the proteins with stoichiometrically bound PLP were then assessed for catalytic activities using the same procedure.

**Preparation of apo-SHMT:** Apo enzymes of SHMT from rabbit and *E. coli* were prepared by a previously reported method, with minor modifications.[75] Approximately 280 µM of holo SHMT was mixed with 0.5 mM EDTA, 1 mM DTT, 200 µM D-alanine and 200 µM ammonium sulfate, in 50 mM potassium phosphate buffer, pH 7. This mixture was incubated at 37 °C with shaking at 150-180 rpm until the yellow color of the holo enzyme disappeared, which indicated removal of PLP from holo-SHMT converting it into apo. This mixture was then dialyzed at 4 °C against 50 mM potassium phosphate buffer, pH 7.5 containing 0.5 mM EDTA and 1 mM DTT. Concentration of apo enzyme was determined from $A_{280\ nm}$. The prepared apo enzyme was stored in aliquots with 10% glycerol at -80 °C if not in use.

**Transfer of PLP from PNPO-PLP complex to apo-SHMT:** Activation of apo-SHMT to holo after transfer of PLP from PNPO-PLP complex was followed at 491 nm, where the ternary complex between glycine, THF and PLP bound to SHMT absorbs maximally. All the reactions were carried out at 37 °C in a 1 cm pathlength thermostated cuvette. 20 µM apo-SHMT (either *E. coli* or rabbit), 50 mM glycine and 100 µM THF were added to 50 mM sodium BES buffer, pH 7. Reaction was started by addition of 20 µM of PNPO-PLP and the activation of SHMT was followed at 491 nm for 15 minutes. Controls were run with 20 µM of free PLP as the source of PLP. In another set of experiments, 3 µM PLP specific phosphatase was added to the reaction mixture prior to addition of PNPO-PLP complex or free PLP. The activation profiles in presence and absence of 3 µM PLP phosphatases were obtained for comparison.

**Test for half site chanelling:** 20 µM apo-eSHMT, 50 mM glycine and 100 µM THF were taken in 50 mM sodium BES buffer, pH 7. Activation reaction of apo-eSHMT was started by addition of 20 µM ePNPO-PLP complex at 37 °C, as mentioned earlier. The reaction was followed until it reached saturation (15 minutes). 20 µM of free PLP was then added to this

reaction mixture and progress of the reaction was followed at 491 nm for another 10 minutes. The same experiment was repeated with 20 µM free PLP replacing ePNPO-PLP complex, as a control. Activation profile of eSHMT was obtained by plotting $A_{491\ nm}$ versus time.

### 3.3 Results and discussions:

**3.3.A Expression and purification of proteins:** All the enzyme preparations were pure, when observed on 10% SDS PAGE of the fractions collected after column purification (Figure 27 a, b, c, d).

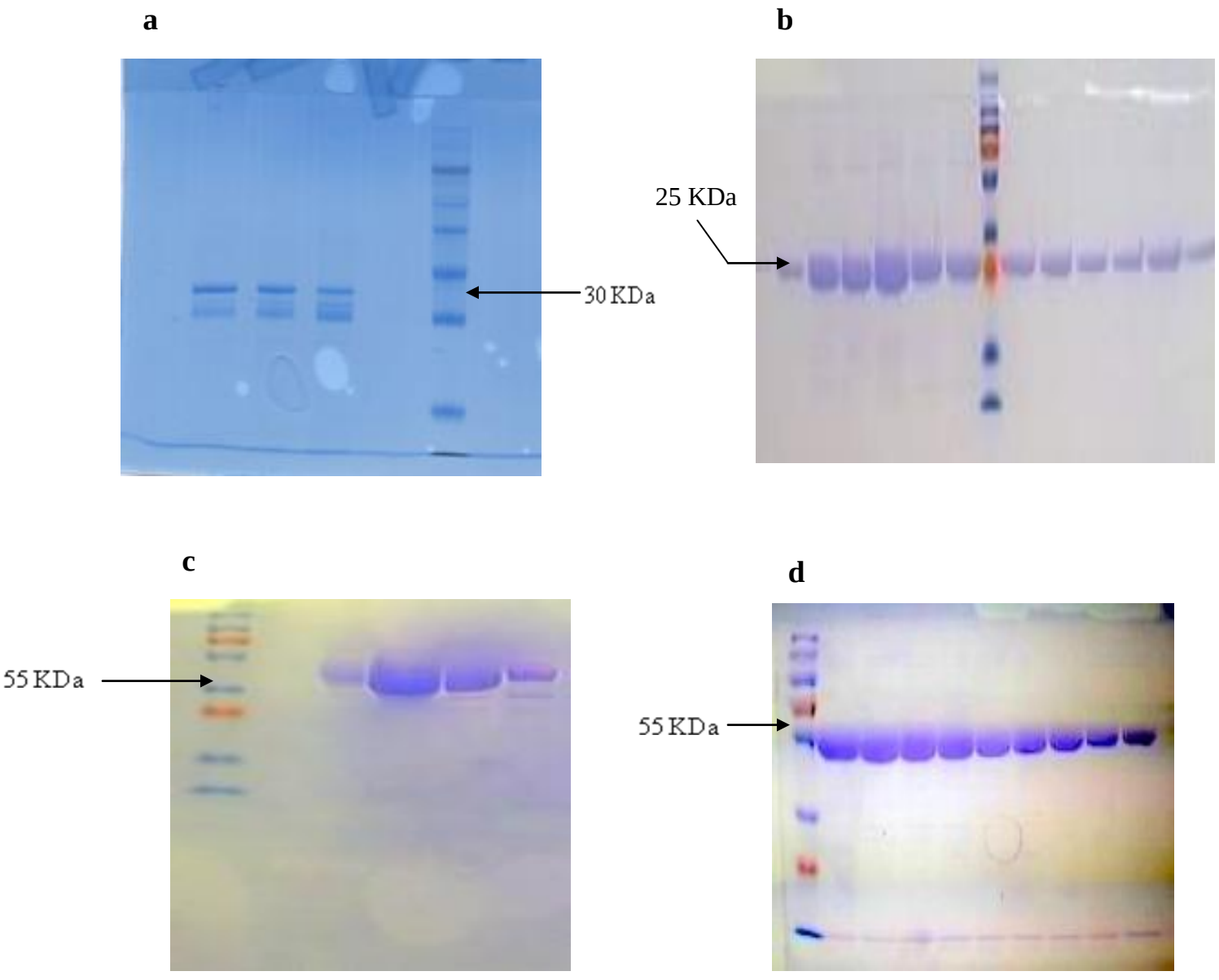


**Figure 27: SDS PAGE of fractions collected after column purification:** (a) human PNPO, (b) *E. coli* PNPO, (c) *E. coli* SHMT and (d) rabbit SHMT

### 3.3.B Determination of mechanism of PLP transfer from PNPO to vitamin $B_6$ dependent enzymes:

#### (a) Affinity pull down assay

The pull down assay was used to determine qualitatively an interaction between human PNPO and rabbit SHMT. Figure 28 shows a picture of the SDS PAGE of the fractions collected after the proteins were loaded onto Ni-NTA as mentioned in Section 3.2.A.I. Lane 1 shows resolution of SDS PAGE ladder (Biorad). Lanes 2 and 3 represent elution profiles of 200 µM rSHMT. Since rSHMT is not His-tagged, the protein did not bind to the Ni-NTA column and was eluted out with the equilibration buffer containing 5 mM imidazole (Lane 2). No protein was eluted out with buffer containing 150 mM imidazole (Lane 3). Lanes 4 and 5 represent binding of 200 µM of human PNPO. Human PNPO bound to Ni-NTA tightly due to the six His residues at the N terminus and therefore was not eluted out with the buffer containing 5 mM imidazole (Lane 4). Increase in imidazole concentration in the buffer to 150 mM eluted out all of the protein (Lane 5). Elution profile for the equimolar mixture of human PNPO and rSHMT is represented by lanes 6 and 7. Some rSHMT was eluted out with 5 mM imidazole in the buffer (Lane 6); whereas passing the buffer containing 150 mM imidazole through the column showed both human PNPO and rSHMT in the eluate (Lane 7). This indicates that there was some interaction between human PNPO and rSHMT due to which the latter remained onto the column even though it is not His tagged.

The experiment was repeated with the non His tagged and non vitamin $B_6$ dependent enzyme lysozyme as a control. Figure 29 shows a picture of SDS PAGE of the fractions collected from the Ni-NTA column. Lane 1 represents resolution of gel marker (Biorad). Lanes 2

and 3 indicate the elution profiles of lysozyme alone. Lysozyme being a non His tagged protein, all of the protein loaded on the Ni-NTA column was eluted out at 5 mM imidazole in the wash buffer (Lane 2). When the concentration of imidazole in the buffer was increased to 150 mM, insignificant amount of imidazole eluted out (Lane 3). This slight binding observed to Ni-NTA in lane 3 may be due to the high non-specificity of lysozyme. When equimolar mixture of lysozyme and human PNPO was loaded onto Ni-NTA column (Lanes 4 and 5), almost all of the lysozyme was eluted at 5 mM imidazole in the buffer (Lane 4). On the other hand elution of the mixture with buffer containing 150 mM imidazole showed band corresponding to human PNPO only, indicating no interaction between lysozyme and human PNPO (Lane 5). The result further confirmed the interaction between PNPO and SHMT to be specific to vitamin $B_6$ dependent enzymes.

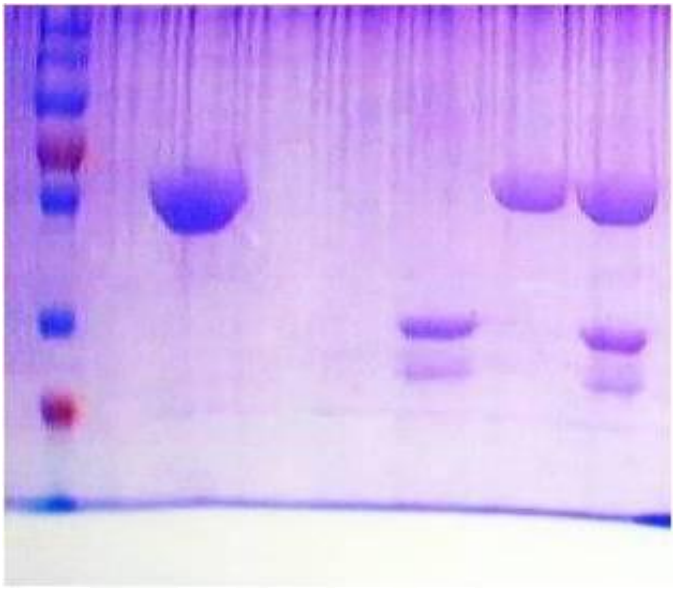


**Figure 28: Pull down experiment with hPNPO and rSHMT:** SDS PAGE analysis of fractions collected from Ni-NTA column (1) Marker; (2) rSHMT wash; (3) rSHMT elution; (4) hPNPO wash; (5) hPNPO elution; (6) Mixture wash; (7) Mixture elution


**Figure 29: Pull down experiment with hPNPO and lysozyme:** SDS PAGE of fractions collected from Ni-NTA column: (1) Marker; (2) Lysozyme wash; (3) Lysozyme elution; (4) Mixture wash; (5) Mixture elution

### (b) Determination of $K_d$ by fluorescence polarization

The technique of fluorescence polarization was used to quantify interactions between human PNPO and several vitamin $B_6$ dependent enzymes. The degree of labelling of human PNPO with FMi was determined from equation 4 and was found to be 1.1 moles of FMi per mole of protein. Also, the enzymatic activity of human PNPO before and after labelling was determined using assay procedure as mentioned in Section 2.2.D. Table 5 shows the rates for the first 60 seconds of the activity assay of both labeled and unlabeled human PNPO. Labelling of human PNPO with the FMi dye did not affect the catalytic activity of the enzyme.

**Table 5:** Initial rates of hPNPO activity (tagged and untagged enzyme)

| | **Initial rate ($min^{-1}$)** |
|---|---|
| **Untagged human PNPO (200 µg)** | 0.3659 |
| **Tagged human PNPO (200 µg)** | 0.36981 |

* Initial rates obtained by following absorption of aldimine formed between product PLP and Tris at 414 nm.

Titration of FMi tagged human PNPO with various vitamin $B_6$ dependent enzymes yields a binding curve of polarization in mP against increasing concentrations of the vitamin $B_6$ depedndent enzymes (Figure 30). Control experiments were run to determine the binding of tagged human PNPO with non-vitamin $B_6$ dependent enzymes, LDH and lysozyme. Saturation binding curves of tagged human PNPO with the vitamin $B_6$ dependent enzymes (Figure 31) clearly show interactions between the proteins as indicated by increase in polarization value with increasing concentrations of the $B_6$ enzymes. On the other hand, no significant change in the

polarization of tagged human PNPO was seen at increasing concentrations of LDH and lysozyme. The experiment demonstrates specificity of binding of human PNPO towards various vitamin $B_6$ dependent enzymes. The dissociation constants ($K_d$) for these bindings were calculated based on Equation 5 and are tabulated in Table 6. All the three enzymes exhibited more or less equal affinity towards hPNPO.

**Table 6:** Dissociation constants ($K_d$) for binding of FMi labeled hPNPO with vitamin $B_6$ dependent enzymes

| **Enzyme** | **$K_d$ (µM)*** |
|---|---|
| rSHMT | 0.8 ± 1.2 |
| eSHMT | 1.3 ± 1.4 |
| AAT | 0.3 ± 0.1 |

* Lower $K_d$ values indicate stronger binding

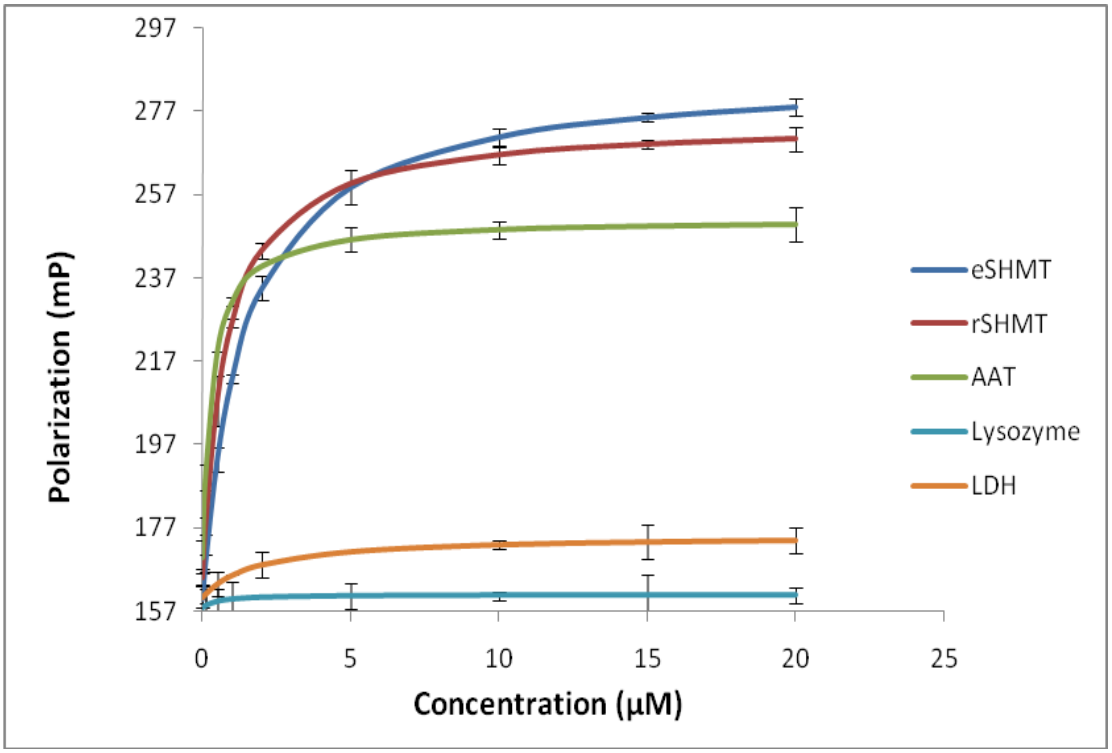


**Figure 30: Saturation binding curves by fluorescence polarization:** Titration of FMi tagged hPNPO with increasing concentrations of: eSHMT (cyan), rSHMT (red), AAT (green), LDH (orange) and lysozyme (blue)

### (c) Kinetic studies of PLP transfer

**Preparation of PNPO-PLP complex:** PNPO-PLP complexes were made with human and *E. coli* proteins as mentioned in Section 3.2.B.c.

**Determination of stoichiometry of PLP binding to PNPO:** Since FMN intereferes with the absorption of PLP at 388 nm, the second method (Section 3.2.B.c) was used to determine the stoichiometry of PLP binding to PNPO. In this method a standard curve was used to analyze the level of PLP released from PNPO-PLP complex (Figure 31). Concentration of PLP bound to PNPO in 30 µM of the complex was determined by extrapolating from the $A_{491\ nm}$ of the complex on the standard curve. Table 7 indicates the concentration of PLP bound to human and *E. coli* PNPO with the stoichiometry of PLP binding to both, which shows that 1 PLP molecule is bound per monomer of PNPO.

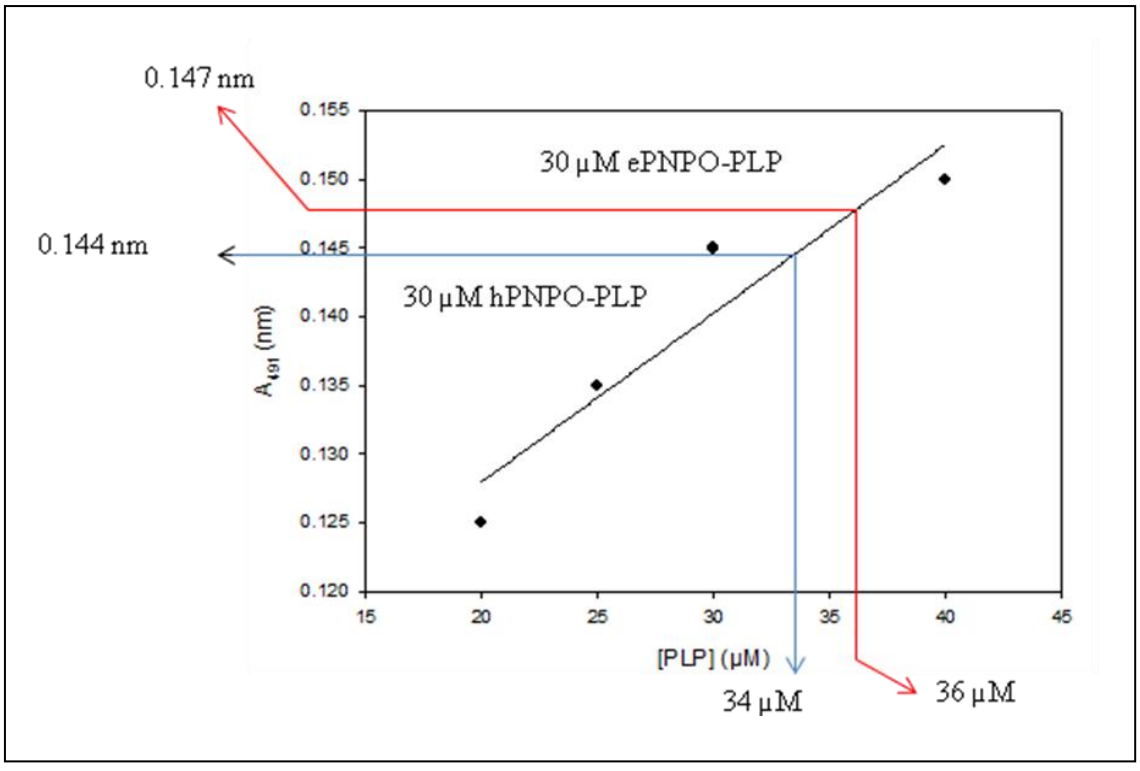


**Figure 31: Stoichiometry of PLP binding to PNPO:** The $A_{491\ nm}$ readings of the quinonoid complex obtained after activation of apo eSHMT by human (blue) and *E. coli* (red) PNPO-PLP complexes are extrapolated on the standard plot

**Table 7:** Stoichiometry of PLP binding to human and *E. coli* PNPO

| | [PLP] in the complex (µM) | Stoichiometry of PLP binding with PNPO $\frac{[PLP]}{[hPNPO - PLP]}$ |
|---|---|---|
| Human PNPO-PLP complex | 34 | 1.13 |
| *E. coli* PNPO-PLP complex | 36 | 1.2 |

**Catalytic activities of PNPO and PNPO-PLP complex:** Both human and *E. coli* enzymes complexed with PLP were assayed along with their uncomplexed forms as references. Table 8 shows the rates of the first 60 seconds of the reaction. There is no significant difference in the catalytic activities of the enzymes in complexed and uncomplexed forms.

**Table 8:** Initial rates of the assay of PNPO (Complexed and uncomplexed enzymes)

| | **Enzyme (200 µg)** | **Initial rate ($min^{-1}$)*** |
|---|---|---|
| **Human PNPO** | PNPO | 0.3765 |
| | PNPO-PLP | 0.3507 |
| ***E. coli* PNPO** | PNPO | 0.4231 |
| | PNPO-PLP | 0.4113 |

* Initial rate of formation of PLP from PNP determined by following formation of aldimine between product PLP and Tris from the buffer at 414 nm

**Transfer of PLP from PNPO-PLP complex to apo-SHMT:** Previous studies have shown that PLP binds tightly to PNPO and is not removed even after extensive dialysis or passage through gel filtration column, consistent with the study reported here[25]. In this study, we followed the transfer of this tightly bound PLP from PNPO to apo-SHMT in the absence and presence of PLP-dependent phosphatase. The rationale behind this experiment was to determine whether the tightly bound PLP in the PNPO-PLP complex is transferable to apo SHMT and also to determine whether the transfer occurs by channeling.

Figure 32 (a) and (b) shows activation profiles of rcSHMT and *E. coli* SHMT respectively with human PNPO-PLP complex. It can be seen that the tightly bound molecule of PLP, which did not separate from PNPO even after dialysis or passage through a gel filtration column, got readily transferred to apo-SHMT. However, the rate of transfer of PLP in the complex form was nearly half of the free form. The experiment was repeated to monitor the transfer of PLP from *E. coli* PNPO-PLP complex to *E. coli* SHMT. (Figure 33) Results were similar to the activation of rcSHMT. It was observed that the transfer of PLP from PNPO-PLP complex to SHMT, when both the complex and apo-SHMT were from the same species or from different species, did not differ significantly. This indicates that the mechanism of PLP transfer is probably similar in all PLP dependent enzymes.

**a**

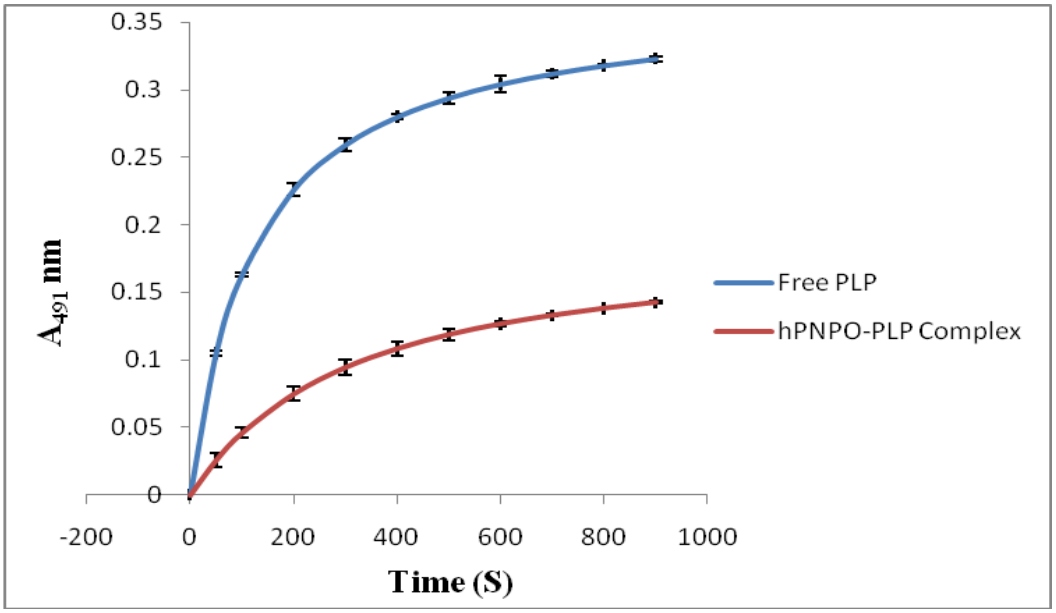


**b**

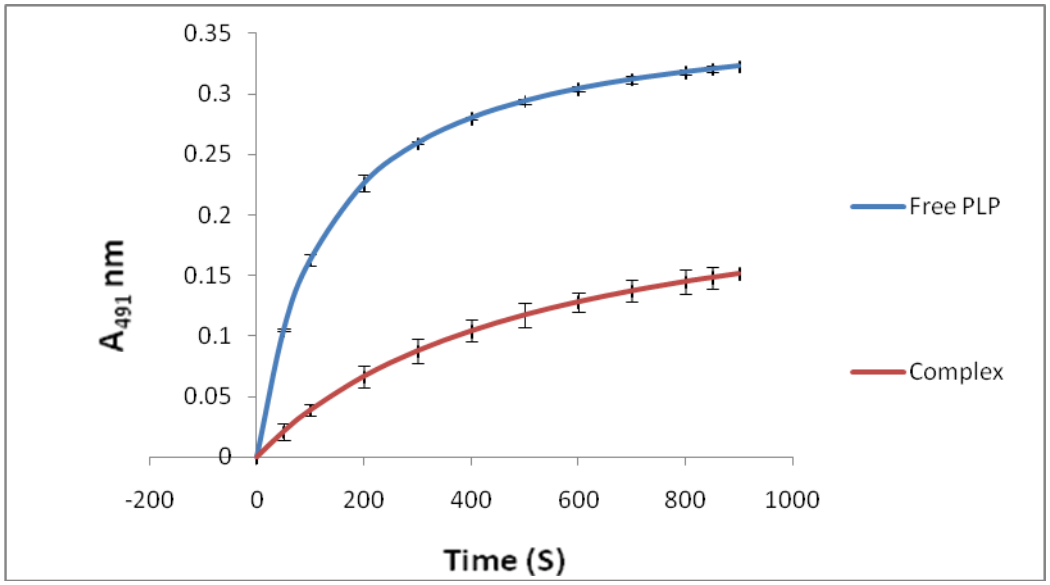


**Figure 32: Activation profile of apo SHMT with hPNPO-PLP complex:** (a) rcSHMT (b) eSHMT; free PLP (blue) and PNPO-PLP complex (red). The results are based on at least two measurements.

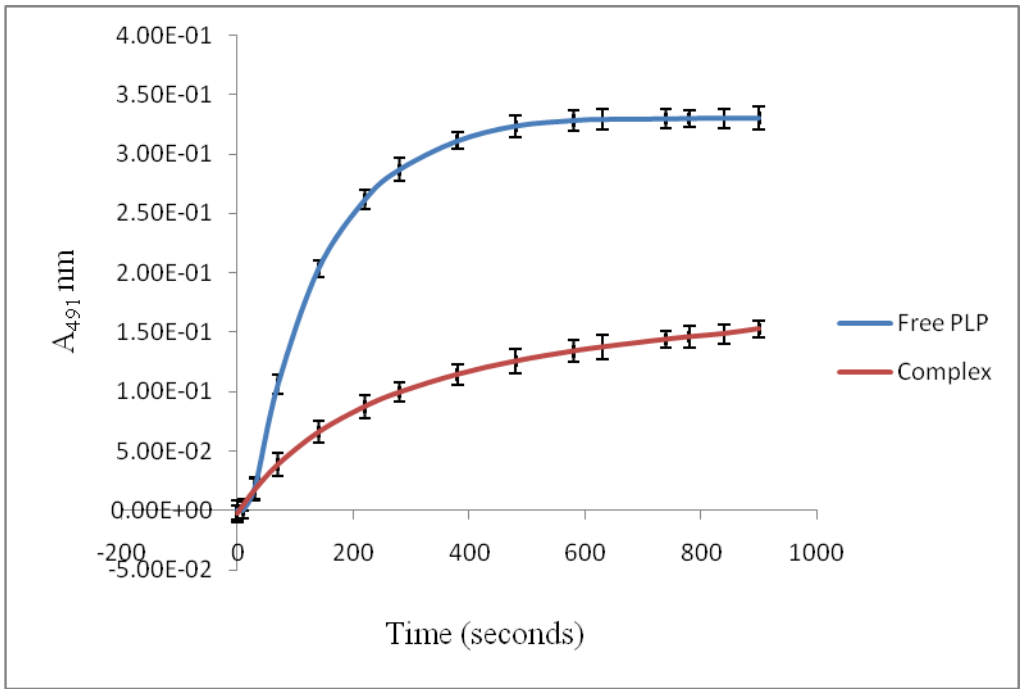


**Figure 33: Activation profile of eSHMT:** With ePNPO-PLP complex(Red); free PLP (blue). The results are based on at least two measurements

**Use of phosphatases:** Phosphatases play a vital role in regulating PLP concentration *in vivo* by converting the phosphorylated forms of $B_6$ vitamers: PNP, PMP and PLP back to PN, PM and PL respectively and account for one of the main reasons for the low concentration of free PLP (~1-3 µM) in the cell.[62] Since this concentration of free PLP is not enough for activating the dozens of apo B6 enzymes, there must be a mechanism for the transfer of PLP synthesized by PNPO and PLK to these apo $B_6$ enzymes. Figure 34 represents the two probable modes of PLP transfer and how the presence of phosphatase can possibly affect this process. PLP phosphatase if present in the reaction mixture would compete with SHMT for the free PLP, thus affecting the rate of activation of apo SHMT. However, in case of channeling, the presence of

phosphatase would not affect activation profile of SHMT since insignificant amount of PLP would be available free in the solution for phosphatase.

Figures 35 (a) and (b) shows the kinetic profiles for activation of 20 µM rc SHMT with 20 µM human as well as *E. coli* PNPO-PLP complexes in presence and absence of 3 µM PLP phosphatase. Activation of apo-SHMT with 20 µM free PLP in presence and absence of PLP phosphatase was also included as a control.

Our study shows that in the presence of PLP-specific phosphatase, the activation of SHMT with free PLP is almost totally inhibited, while it has no significant effect on the transfer of the tightly bound PLP on the oxidase. This shows that phosphatase did not convert the PLP back to PL when the complex was used for activation, which indicates that PLP may not be released into the solution and remains attached to PNPO until it is transferred to SHMT. Channeling, thus, seems to be the probable mechanism for transfer of PLP from PNPO to SHMT.

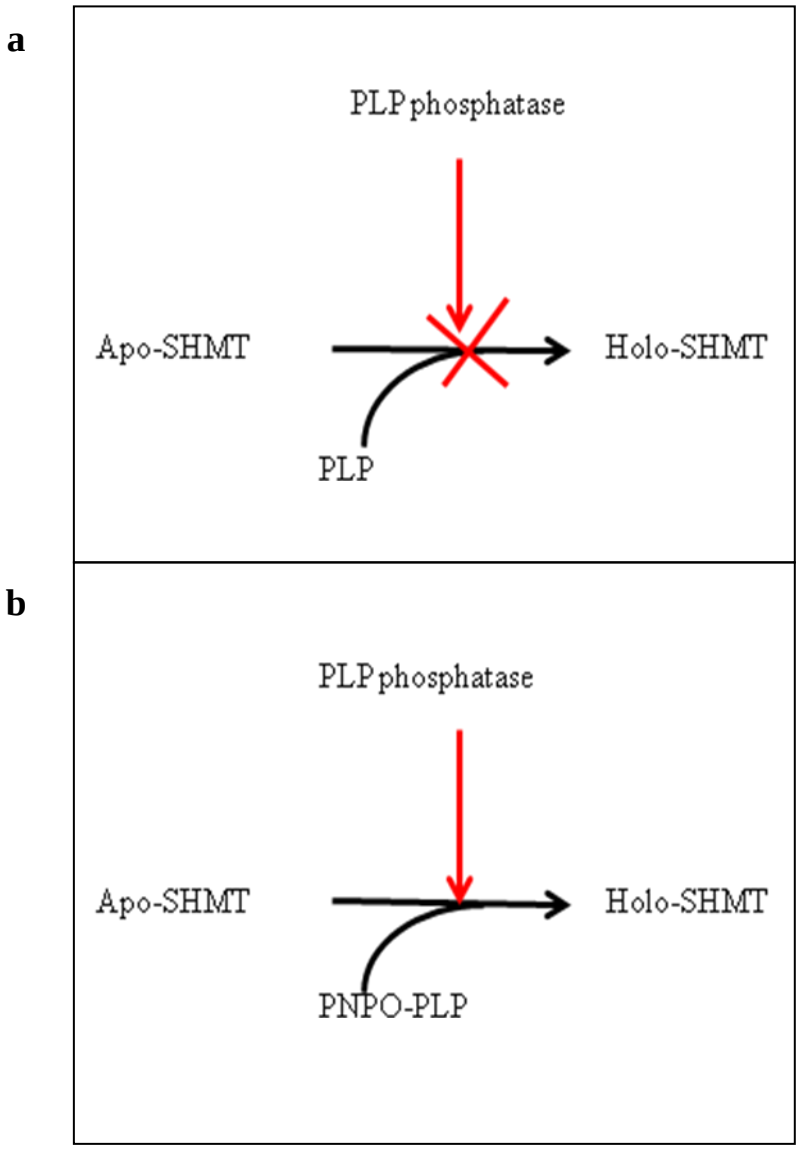


**Figure 34: Effect of PLP phosphatase on transfer of PLP:** (a) in the free form after PNPO releases it and (b) complexed to PNPO which gets transferred to apo-SHMT via channeling

**a**

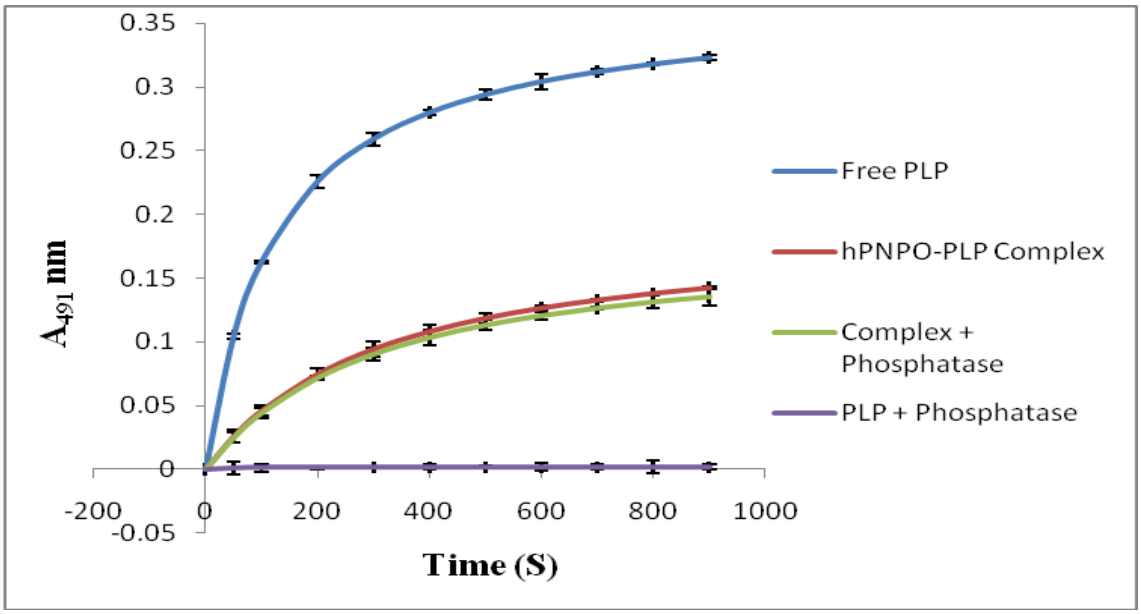


**b**

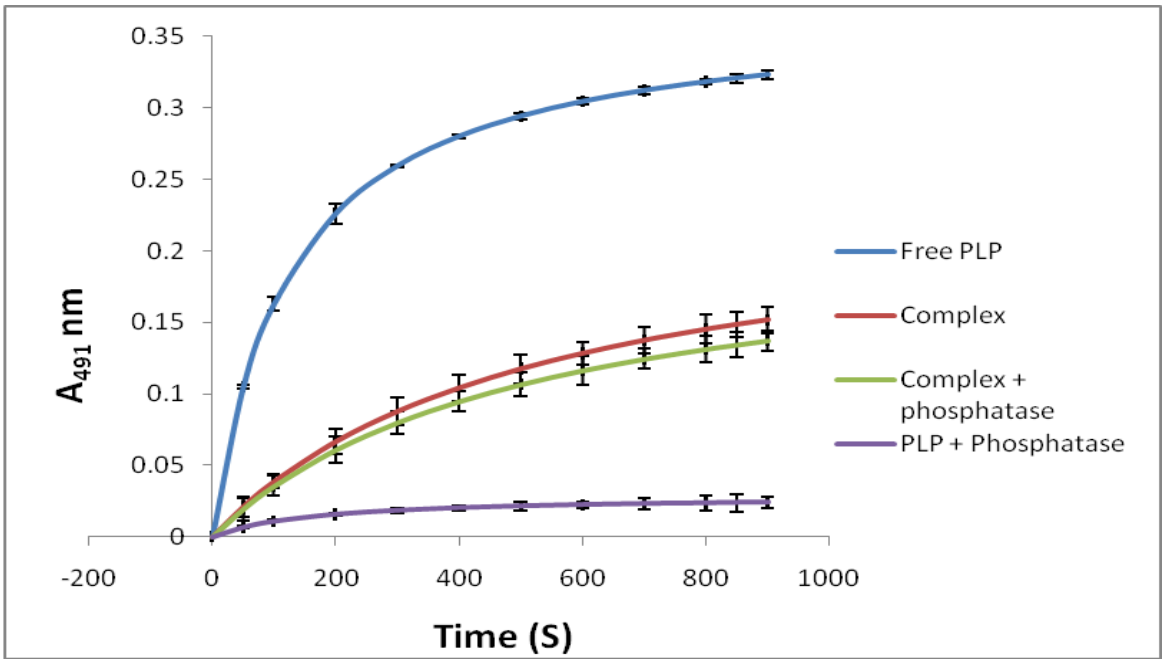


**Figure 35: Activation profile of apo SHMT with hPNPO in presence of PLP phosphatase:** (a) apo rcSHMT and (b) apo eSHMT activation with hPNPO-PLP complex; free PLP (blue), hPNPO-PLP complex (red), complex in presence of phosphatase (green) and free PLP in presence of phosphatase (purple)

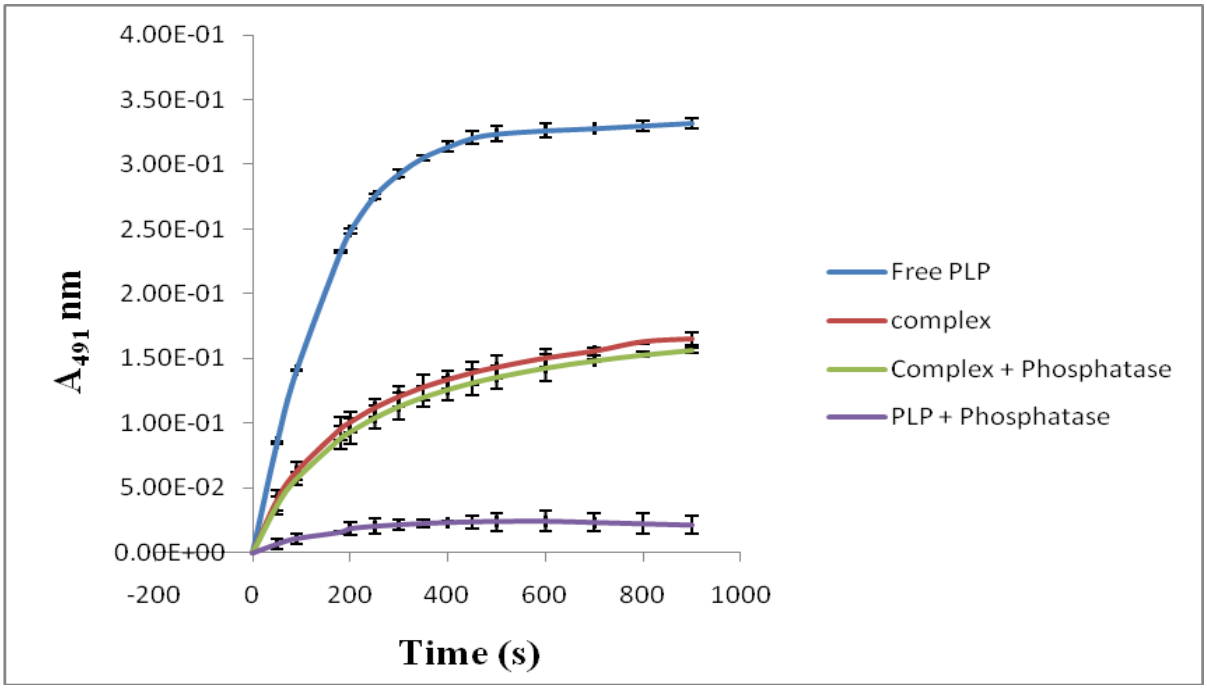


**Figure 36: Activation profile of apo eSHMT with ePNPO-PLP complex in presence of PLP phosphatase:** Free PLP (blue), complex (red), complex in presence of phosphatase (green), free PLP in presence of phosphatase (purple)

**Test for half site chanelling:** The rate of formation of ternary quinonoid comlpex with PNPO-PLP complex was observed to be nearly half as compared to the activation with free PLP under the assay conditions. This could be explained by the phenomenon of half site channeling, where either one of the interacting enzymes, (PNPO and SHMT) shares only one PLP binding site in the interaction, i. e. either PNPO-PLP complex might be sharing only one PLP binding site with apo SHMT or SHMT makes only one site available for PLP from the complex. Figure 37 shows the observed activation profile of eSHMT. The rate of formation of ternary complex showed a sharp rise on addition of additional 20 µM of free PLP to PNPO-PLP complex. On the other hand addition of free PLP to the reaction with free PLP did not show any difference in the

rate. This indicates that the transfer of PLP from PNPO-PLP to SHMT possibly occurs via half site channeling under the assay conditions in 50 mM sodium BES buffer, pH 7.

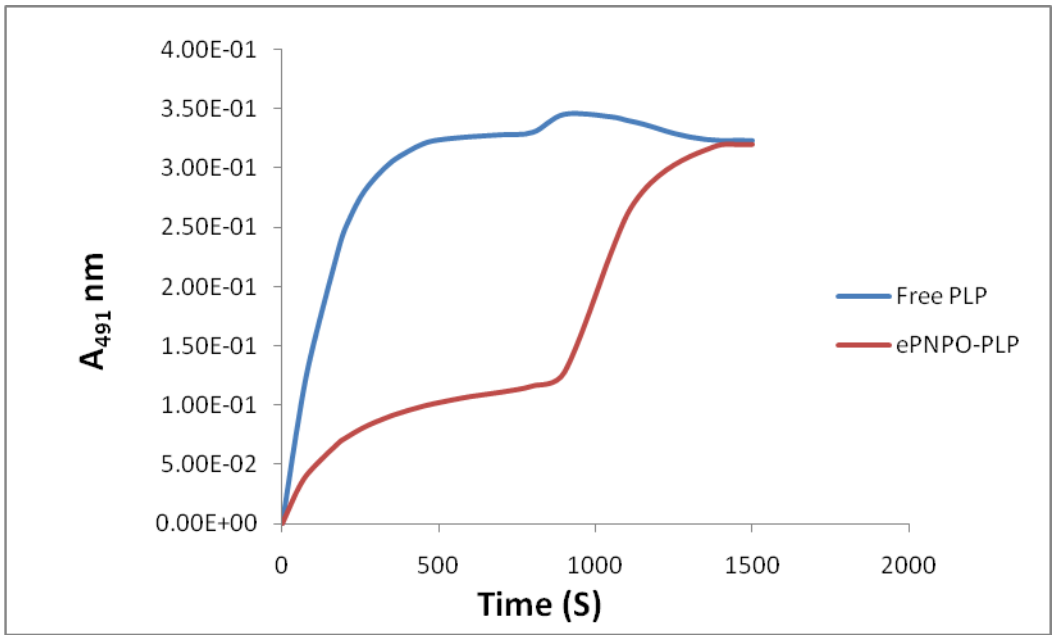


**Figure 38: Test for half site channeling:** ePNPO-PLP complex (Red); free PLP (Blue)

**3.4 Conclusions:** PNPO interacts with the vitamin $B_6$ dependent enzymes as observed from the affinity pull down experiment and the interaction is specific as no interaction was observed between PNPO and the non vitamin $B_6$ dependent enzyme, e.g. lysozyme. Furthermore, the interaction exhibits nanomolar to submicromolar range of the dissociation constants ($K_d$) between PNPO and $B_6$ enzymes using fluorescence polarization, indicating high affinity between the interacting proteins. This supported the possibility of channeling as a probable mechanism of transfer of PLP. In order to further investigate the mode of transfer of PLP we performed kinetic studies which showed that the PLP from PNPO-PLP complex (which was unremovable during extensive dialysis or passage through column) was readily transferred to apo SHMT. This transfer was not affected by the presence of PLP phosphatase which indicates the release of free PLP into the solution by PNPO is unlikely. The rate of activation by the complex was nearly half of free PLP. Addition of free PLP after the activation with complex reached saturation, supports the possibility of half site channeling.

## LITERATURE CITED


1. McCormick, D. B.; Chen, S. Update on interconversions of vitamin $B_6$ with its coenzyme. *J. Nutr*. **1999**, *129*, 325-327.
2. Mittenhuber, G. Phylogenic analysis and comparative genomics of vitamin $B_6$ (pyridoxine) and pyridoxal phosphate biosynthesis pathways. *J. Mol. Microbiol. Biotechnol.* **2001**, *3*, 1-20.
3. Dempsey, W. B. Control of pyridoxine biosynthesis in *Escherichia coli*. *J.Bacteriol.* **1965**, *90*, 431-437.
4. Fu, T.; di Salvo, M.; Schirch, V. Distribution of $B_6$ vitamers in *Escherichia coli* as determined by enzymatic assay. *Anal. Biochem.* **2001**, *298*, 314-321.
5. Lam, H.; Winkler, M. Metabolic relationships between pyridoxine (vitamin $B_6$) and serine biosynthesis in *Escherichia coli* K-12. *J. Bacteriol.* **1990**, *172*, 6518-6528.
6. Hill, R.E.; Himmeldirk, K.; Kennedy, I. A.; Pauloski, R. M.; Sayer, B.G.; Wolf, E.; Spenser, I. D. The biogenetic anatomy of vitamin $B_6$. *J. Biol. Chem.* **1996**, *271*, 30426-30435.
7. Li, T. K.; Lumeng, L.; Veitch, R. L. Regulation of pyridoxal 5'-phosphate metabolism in liver. *Biochem. Biophys. Res. Commun.* **1974**, *61*(2), 677-684.
8. McCormick, D. B.; Gregory, M. E.; Snell, E. E. Pyridoxal phosphokinase I: assay, distribution, purification and properties. *J. Biol. Chem.* **1961**, *236*, 2076-2084.
9. Musayev, F. N.; di Salvo, M. L.; Ko, T. Z.; Gandhi, A. K.; Goswami, A.; Schirch, V.; Safo, M. K. Crystal structure of human pyridoxal kinase: Structural basis of $M^+$ and $M^{2+}$ activation. *Prot. Sci.* **2007**, *16*, 2184-2194.

10. Di Salvo, M. L.; Hunt, S.; Schirch, V. Expression, purification and kinetic constants for human and *Escherichia coli* pyridoxal kinases. *Prot. Exp. Pur.* **2004**, *36*, 300-306.
11. Safo, M. K.; Musayev, F. N.; Hunt, S. di Salvo, M. L.; Scarsdale, N.; Schirch, V. Crystal structure of the PdxY protein from Escherichia coli. *J. Bacteriol.* **2004**, *186*, 8074-8082.
12. Safo, M. K.; Musayev, F. N.; di Salvo, M. L.; Hunt, S.; Claude, J. B.; Schirch, V. Crystal structure of pyridoxal kinase from *Escherichia coli* PdxK gene: Implications for the classification of pyridoxal kinases. *J. Bacteriol*. **2006**, *188*, 4542-4552.
13. Li, M. H.; Kwok, F.; Chang, W. R.; Lau, C. K.; Zhang, J. P.; Lo, S. C.; Jiang, T.; Liang, D. C. Crystal structure of brain pyridoxal kinase, a novel member of ribokinase superfamily. *J. Biol. Chem.* **2002**, *277*, 46285-46390.
14. Li, M. H.; Kwok, F.; Chang, W. R.; Lau, C. K.; Zhang, J. P.; Lo, S. C.; Jiang, T.; Liang, D. C. Conformational changes in the raction of pyridoxal kinase. *J. Biol. Chem.* **2004**, *279*, 17459-17465.
15. Di Salvo, M.; Yang, E.; Zhao, G.; Winkler, M. E.; Schirch, V. Expression, purification and characterization of recombinant *Escherichia coli* pyridoxine 5'-phosphate oxidase. *Prot. Exp. Purif.* **1998**, *13*(3), 349-356.
16. Musayev, F. N.; Di Salvo, M. L.; Ko, T. P.; Schirch, V.; Safo, M. K. Structure and properties of recombinant human pyridoxine 5'-phosphate oxidase. *Prot. Sci.* **2003**, *12*, 1455-1463.
17. Di Salvo, M. L.; Safo, M. K.; Musayev, F. N.; Bossa, F.; Schirch, V. Structure and mechanism of *Escherichia coli* pyridoxine 5'-phosphate oxidase. *Biochim. Biophys. Act.* **2003**, *1647*, 76-82.

18. Zhao, G.; Winkler, M. E. Kinetic limitation cellular amount of pyridoxine (pyridoxamine) 5'-phosphate oxidase of *Escherichia coli* K-12. *J. Bacteriol.* **1995**, *177*, 883-891.

19. Safo, M. K.; Musayev, F. N.; Di Salvo, M. L.; Schirch, V. X-ray structure of *Escherichia coli* pyridoxine 5'-phosphate oxidase complexed with pyridoxal 5'-phosphate at 2.0 Å resolution. *J. Mol. Biol.* **2001**, *310*, 817-826.

20. Safo, M. K.; Mathews, I.; Musayev, F. N.; Di Salvo, M. L.; Thiel, D. J.; Abraham, D. J.; Schirch, V. X-ray structure of *Escherichia coli* pyridoxine 5'-phosphate oxidase complexed with FMN at 1.8 Å resolution. *Stru.* **2000,** *8*, 751-762.

21. Kazarinoff, M. N.; McCormick, D. B. Rabbit liver pyridoxine (pyridoxamine) 5'-phosphate oxidase: purification and properties. **1975**, *250*, 3436-3442.

22. Choi, S. Y.; Churchich, J. E.; Zaiden, E.; Kwok, F. Brain pyridoxine 5'-phosphate oxidase: Modulation of its catalytic activity by reaction with pyridoxal 5'-phosphate and analogs. *J. Biol. Chem.* **1987**, *262*, 12013-12017.

23. Lui, A.; Lumeng, L.; Li, T. K. Mitochondrial vitamin $B_6$ metabolism. *J. Biol. Chem.* **1981**, *256*, 6041-6046.

24. Di Salvo, M. L.; Ko, T. P.; Musayev, J. N.; Raboni, S.; Schirch, V.; Safo, M. K.; Active site structure and stereospecificity of *Escherichia coli* pyridoxine 5'-phosphate oxidase. *J. Mol. Biol.* **2002**, *315*, 385-397.

25. Yang, E. S.; Schirch, V. Tight binding of pyridoxal 5'-phosphate to recombinant *Escherichia coli* pyridoxine 5'-phosphate oxidase. *Arch. Biochem. Biophys.* **2000**, *377*, 109-114.

26. Eliot, A. C.; Kirsch, J. F. Pyridoxal phosphate enzymes: Mechanistic, structural and evolutionary considerations. *Ann. Rev. Biochem.* **2004**, *73*, 383-415.

27. John, R. A. Pyridoxal phosphate-dependent enzymes. *Biochim. Biophys. Act.* **1995**, *1248*, 81-96.

28. McCormick, D. B. Biochemistry of coenzymes. In encyclopedia of molecular biology and molecular medicine (Meyers. R. A., ed.), 1996, pp. 396-406, VCH. Weinheim, Germany.

29. Leklem, J. E. Vitamin $B_6$ in handbook of vitamins (Machlin, L. ed.), **1991**, pp. 341-378, Marcel Decker Inc. New York.

30. Jansonius, J. N. Structure, evolution and action of vitamin $B_6$ dependent enzymes. *Curr. Opin. Stru. Biol.* **1998**, *8*, 759-769.

31. Bohme, I.; Luddens, H. The inhibitory neural circuitry as target of antiepileptic drugs. *Curr. Med. Chem.* **2001**, *8*, 1257-1274.

32. Butterworth, J.; Yates, C. M.; Simpson, J. Phosphate activated glutaminase in relation to Huntington's disease and agonal state. *J. Neurochem.* **1983**, *41*, 440-447.

33. Snyder, S. H.; Ferris, C. D. Novel neurotransmitters and their neuropsychiatric relevance. *Am. J. Psychiatry.* **2000**, *157*, 1738-1751.

34. Schrag, A. Psychiatric aspects of Parkinson's disease- an update. *J. Neurol.* **2004**, *251*, 795-804.

35. Lloyd, K. G.; Munari, C.; Worms, P.; Bossi, L.; Bancaud, J.; Talairach, J.; Morselli, Pl. L. The role of GABA mediated neurotransmission in convulsive states. *Adv. Biochem. Psychopharmacol.* **1981**, *26*, 199-206.

36. Nishino, N.; Fujiwara, H.; Noguchi-Kuno, S. A.; Tanaka, C. GABA-A receptor but not muscarinic receptor density was decreased in the breain of patients with Parkinson's disease. *Jpn. J. Pharmacol.* **1988**, *48*, 331-339.

37. Aoyagi, T.; Wada, T.; Nagai, M.; Kojima, F.; Harada, S.; Takeuchi, T.; Takahashi, H.; Hirokawa, K.; Tsumita, T. Increased gamma-aminobutyrate aminotransferase activity in brain of patients with Alzheimer's disease. *Chem. Pharm. Bull. (Tokyo)*, **1990**, *38*, 1748-1749.

38. Haas, H.; Panula, P. The role of histamine and the tubermamillary nucleus in nervous system. *Nat. Rev. Neurosci.* **2003**, *4*, 121-130.

39. Ohtsu, H.; Watanabe, T. New functions of histamine found in histidine decarboxylase gene knockout mice. *Biochem. Biophys. Res. Commun.* **2003**, *305*, 443-447.

40. Salva, A.; Donoso, J.; Frau, J.; Munoz, F. Theoretical studies on Schiff base formation of vitamin $B_6$ analogues. *J. Mol. Stru. (Theochem).* **2002**, *577*, 229-238.

41. Toney, M. D. Reaction specificity in pyridoxal phosphate enzymes. *Arch. Biochem. Biophys.* **2005**, *433*, 279-287.

42. Mehta, P. K.; Christen, P. The molecular evolution of pyridoxal 5'-phosphate dependent enzymes. *Adv. Enzymol. Relat. Areas. Mol. Biol.* **2000**, *74*, 129-184.

43. Christen, P.; Mehta, P. K. From cofactors to enzymes: The molecular evolution of pyridoxal 5'-phosphate dependent enzymes. *Chem. Rec.* **2001**, *1*, 436-447.

44. Grishin, N. V.; Phillips, M. A.; Goldsmith, E. J. Modeling of the spatial structure of eukaryotic ornithine decarboxylases. *Prot. Sci.* **1995**, *4*, 1291-1304.

45. Clayton, P. T. $B_6$ responsive disorders: a model of vitamin dependency. *J. Inherit. Metab.* **2006**, *29*, 317-326.

46. Morris, M. S.; Picciano, M. F.; Jaques, P. F.; Selhub, J. Plasma pyridoxal 5'-phosphate in the US population: The National Health and Nutrition Examination Survey, 2003-2004. *Am. J. Clin. Nutr.* **2008**, *87*, 1446-1454.

47. McCormick, D. B.; Snell, E. E. Pyridoxal kinase from bacteria and from mammalian tissues. In methods in enzymology (Colowick, S. P.; Kaplan, N. O., ed), **1970**, pp. 611-623, Part A. Academic Press, New York.

48. Kortnyk, W.; Hakala, M. T.; Potti, P. G.; Angelino, N.; Cheng, S. C. On the inhibitory activity of 4-vinyl analogues of pyridoxal: Enzyme and cell culture studies. *Biochem.* **1976**, *15*, 5458-5466.

49. Laine-Cessac, P.; Cailleux, A.; Allain, P. Mechanisms of inhibition of human erythrocyte pyridoxal kinase by drugs. *Biochem. Pharmacol.* **1997**, *54*, 863-870.

50. Seto, T.; Inada, H.; Kobayashi, N.; Tada, H.; Furukawa, K.; Hayashi, K.; Hattori, H.; Matsuoka, O.; Isshiki, G. Depression of serum pyridoxal levels in theophylline-related seizures. *No to Hattatsu.* **2000**, *32*, 295-300.

51. Adams, P. W.; Folkard, J.; Wynn, V.; Seed, M. Influence of oral contraceptives, pyridoxine (vitamin $B_6$), and tryptophan on carbohydrate metabolism. *Lanc.* **1976**, *1*, 759-764.

52. Lumeng, L.; Li, T. K. Vitamin $B_6$ metabolism in chronic alcohol abuse. Pyridoxal phosphate levels in plasma and the effects of acetaldehyde on pyridoxal phosphate synthesis and degradation in human erythrocytes. *J. Clin. Invest.* **1974**, *53*, 693-704.

53. Aaltonen, J.; Bjorses, P.; Sandkuijl, L.; Perheentupa, J.; Peltonen, L. An autosomal locus causing autoimmune disease: autoimmune polyglandular disease type I assigned to chromosome 21. *Nat. Genet.* **1994**, *8*, 83-87.

54. Mills, P. B.; Surtees, A. H.; Champion, M. P.; Beesley, C. E. Dalton, N.; Scambler, P. J.; Heales, S. J. R.; Zschocke, J.; Clayton, P. T. Neonatal epileptic enxephalopathy caused by mutations in the PNPO gene encoding pyridox(am)ine 5'-phosphate oxidase. *Hum. Mol. Gen.* **2005**, *14(8)*, 1077-1086.

55. Sandyk, R.; Pardeshi, R. Pyridoxine improves drug induced parkinsonism and psychosis in a schizophrenic patient. *Int. J. Neurosci.* **1990**, *52*, 225-232.

56. Nogovitsina, O. R.; Levitina, E. V. Effect of MAGNE-$B_6$ on the clinical and biochemical manifestations of the syndrome of attention deficit and hyperactivity in children. *Eksp. Klin. Farmakol.* **2006**, *69*, 74-77.

57. Ruiz, A.; Garcia-Villoria, J.; Ormazabal, A.; Zschocke, J.; Fiol, M.; Navarro-Sastre, A.; Artuch, R.; Vilaseca, M. A.; Ribes, A. A new fatal case of pyridox(am)ine 5'-phosphate oxidase (PNPO) deficiency. *Mol. Genet. Metab.* **2008**, *93*, 216-218.

58. Scott, K.; Zerris, S.; Kothari, M. J. Elevated $B_6$ levels and peripheral neuropathies. *Electromyogr. Clin. Neurophysiol.* **2008**, *48*, 219-233.

59. Foca, F. J. Motor and sensory neuropathy secondary to excessive pyridoxine ingestion. *Arch. Phys. Med. Rehabil.* **1985**, *66*, 634-636.

60. Anthopol, W.; Tarlov, I. M. Experimental study of the effects produced by large doses of vitamin $B_6$. *J. Neuropathol. Exp. Neurol.* **1942**, *1*, 330-336.

61. Krinke, G.; Schaumburg, H. H.; Spencer, P. S.; Suter, J.; Thomann, P.; Hess, R. Pyridoxine megavitaminosis produces degeneration of peripheral sensory neurons (sensory neuropathy) in the dog. *Neurotoxicol.* **1980**, *2*, 13-24.

62. Jang, Y. M.; Kim, D. W.; Kang, T. C.; Won, M. H.; Baek, N. I.; Moon, B. J.; Choi, S. Y.; Kwon, O. S. Human pyridoxal phosphatase: molecular cloning, functional expression, and tissue distribution. *J. Biol. Chem.* **2003**, *278*, 50040-50046.

63. Shwartz, R.; Kjelgaard, N. O. The enzymatic oxidation of pyridoxal by liver aldehyde oxidase. *Biochem.* **1950**, *48*, 333-337.

64. Stanulovic, M.; Jeremic, V.; Leskovac, V.; Chaykin, S. New pathway of conversion of pyridoxal to 4-pyridoxic acid. *Enz.* **1976**, *21*, 357-369.

65. Churchich, J. E.; Farrelly, J. G. Mechanism of binding of pyridoxamine 5'-phosphate to apoenzyme aspartate aminotransferase: fluorescence studies. *J. Biol. Chem.* **1969**, *244*, 3685-3690.

66. Kwok, F.; Churchich, J. E. Brain pyridoxal kinase. Purification, substrate specifities, and sensitized photodestruction of an essential histidine. *J. Biol. Chem.* **1979**, *254*, 6489-6495.

67. Kim, Y. T.; Churchich, J. E. Activation of a flavoprotein by proteolysis. *J. Biol. Chem.* **1989**, *264*, 15751-15753.

68. Clayton, P. T.; Surtees, R. A.; DeVile, C.; Hyland, K.; Heales, S. J. Neonatal epileptic encephalopathy. *Lancet* **2003**, *361*, 1614-1614.

69. Musayev, F. N.; Di Salvo, M. L.; Saavedra, M. A.; Contestabile, R.; Ghatge, M. S.; Haynes, A.; Schirch, V.; Safo, M. K. Molecular basis of reduced pyridoxine 5'-phosphate oxidase catalytic activity in neonatal epileptic encephalopathy disorder. *J. Biol. Chem.* **2009**, *284*, 30949-30956.

70. Khayat, M.; Korman, S. H.; Frankel, P.; Weintraub, Z.; Herschkowitz, S.; Sheffer, V. F.; Ben Elisha, M.; Wevers, R. A.; Falik-Zaccai, T. C. PNPO deficiency: An under diagnosed inborn error of pyridoxine metabolism. *Mol. Genet. Metab.* **2008**, *94*, 431-434.

71. Bagci, S.; Zschocke, J. Hoffmann, G. F.; Bast, T.; Klepper, J.; Muller, A.; Heep, A.; Bartmann, P.; Franz, A. R. Pyridoxal phosphate-dependent neonatal epileptic encephalopathy. *Arch. Dis. Child. Fetal Neonat. Ed.* **2008**, *93*, F151-152.

72. Hoffmann, G. F.; Schmitt, B.; Windfuhr, M. Pyridoxal 5'-phosphate may be curative in early-onset epileptic encephalopathy. *J. Inherit. Metab. Dis.* **2007**, *30*, 96-99.

73. Tsuge, H.; Ozeki, K.; Ohashi, K. Molecular and enzymatic properties of pyridoxamine (pyridoxine) 5'-phosphate oxidase from baker's yeast. *Agric. Biol. Chem.* **1980**, *44*, 2329-2335.

74. Di Salvo, M. L.; Fratte, S. D.; Biase, D. D.; Bossa, F.; Schirch, V. Purification and characterization of recombinant rabbit cytosolic serine hydroxymethyltransferase. *Prot. Exp. Purific.* **1998**, *13*, 177-183.

75. Schirch, V.; Hopkins, S.; Villar, E.; Angelaccio, S. Serine hydroxymethyltransferase from *Escherichia coli*: purification and properties. *J. Bacteriol.* **1985**, *163*, 1-7.

76. Nasir, M. S.; Jolly, M. E. Fluorescence polarization: an analytical tool for immunoassay and drug discovery. *Comb. Chem. High Throughput Screen.* **1999**, *2*, 177-190.

77. Chen, M. S.; Schirch, V. Serine hydroxymethylase: studies on the role of tetrahydrofolate. *J. Biol. Chem.* **1973**, *248*, 7979-7984.

78. Schirch, V. Serine hydroxymethylase: relaxation and transient kinetic study of the formation and interconversion of the enzyme-glycine complexes. *J. Biol. Chem.* **1975**, *250*, 1939-1945.

79. Trivedi, V.; Gupta, A.; Jala, V. R.; Saravanan, P.; Rao, G. S. J.; Rao, N. A.; Savithri, H. S.; Subramanya, H. S. Structure of binary and ternary complexes of serine hydroxymethyltransferase from *Bacillus stearothermophilus*. *J. Biol. Chem.* **2002**, *277*, 17161-17169.

80. Boe A. S.; Bredholt G.; Knappskog P. M.; Storstein A.; Vedeler C. A.; Husebye E. S. Pyridoxal phosphatase is a novel cancer autoantigen in the central nervous system. British Journal of Cancer, 2004, 91, 1508-1514.